(12) INTERNATIONAL APPLICATION PUBLISHED UNDER THE PATENT COOPERATION TREATY (PCT)

(19) World Intellectual Property Organization
International Bureau

(43) International Publication Date
8 July 2004 (08.07.2004)

PCT

(10) International Publication Number
WO 2004/057393 A1

(51) International Patent Classification[7]: G02B 6/16, 6/20, C03B 37/012

(21) International Application Number: PCT/GB2003/005666

(22) International Filing Date: 22 December 2003 (22.12.2003)

(25) Filing Language: English

(26) Publication Language: English

(30) Priority Data:
0229826.3 20 December 2002 (20.12.2002) GB
0302632.5 5 February 2003 (05.02.2003) GB

(71) Applicant *(for all designated States except US)*: **BLAZEPHOTONICS LIMITED** [GB/GB]; Finance Office, University of Bath, The Avenue, Claverton Down, Bath BA2 7AY (GB).

(72) Inventors; and

(75) Inventors/Applicants *(for US only)*: **WILLIAMS, David, Philip** [GB/GB]; Flat 7, 27 Marlborough Buildings, Bath BA1 2LY (GB). **ROBERTS, Peter, John** [GB/GB]; 11 Gladstone Road, Bath BA2 5HJ (GB). **SABERT, Hendrik** [DE/GB]; Flat 2, 19 Royal Crescent, Bath BA1 2LT (GB). **BIRKS, Timothy, Adam** [GB/GB]; 14 Horsecombe Brow, Combe Down, Bath BA2 5QY (GB). **MANGAN, Brian, Joseph** [GB/GB]; 20 Prior Park Road, Bath BA2 4NG (GB). **KNIGHT, Jonathan, cave** [GB/GB]; Canteen Cottage, Canteen Lane, Wellow, Bath BA2 8PY (GB). **RUSSELL, Philip, ST.John** [GB/GB]; Shepherds Mead, Southstoke, Bath BA2 7EB (GB).

(74) Agents: **CRITTEN, Matthew, Peter** et al.; Abel & Imray, 20 Red Lion Street, London WC1R 4PQ (GB).

(81) Designated States *(national)*: AE, AG, AL, AM, AT, AU, AZ, BA, BB, BG, BR, BW, BY, BZ, CA, CH, CN, CO, CR, CU, CZ, DE, DK, DM, DZ, EC, EE, EG, ES, FI, GB, GD, GE, GH, GM, HR, HU, ID, IL, IN, IS, JP, KE, KG, KP, KR, KZ, LC, LK, LR, LS, LT, LU, LV, MA, MD, MG, MK, MN, MW, MX, MZ, NI, NO, NZ, OM, PG, PH, PL, PT, RO, RU, SC, SD, SE, SG, SK, SL, SY, TJ, TM, TN, TR, TT, TZ, UA, UG, US, UZ, VC, VN, YU, ZA, ZM, ZW.

(84) Designated States *(regional)*: ARIPO patent (BW, GH, GM, KE, LS, MW, MZ, SD, SL, SZ, TZ, UG, ZM, ZW), Eurasian patent (AM, AZ, BY, KG, KZ, MD, RU, TJ, TM),

[Continued on next page]

(54) Title: PHOTONIC BAND-GAP OPTICAL FIBER WITH LARGE HOLLOW CORE

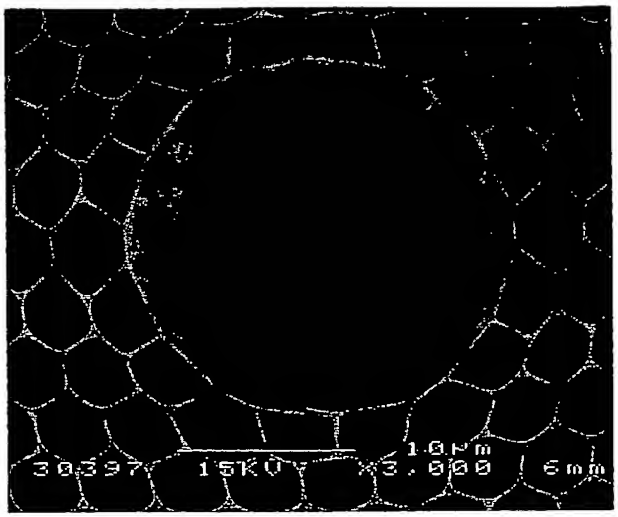

(57) Abstract: The present invention is in the field of photonic band-gap optical fibres and, in particular, hollow core photonic band-gap optical fibres. The present inventors describe examples of such fibres that guide light by virtue of a true photonic band-gap in a relatively large hollow core region. The inventors show that such fibres can exhibit surprising characteristics and that, for example, modes supported by the large hollow core region can be tuned by modifying the form of the core boundary region.

WO 2004/057393 A1

European patent (AT, BE, BG, CH, CY, CZ, DE, DK, EE, ES, FI, FR, GB, GR, HU, IE, IT, LU, MC, NL, PT, RO, SE, SI, SK, TR), OAPI patent (BF, BJ, CF, CG, CI, CM, GA, GN, GQ, GW, ML, MR, NE, SN, TD, TG).

For two-letter codes and other abbreviations, refer to the "Guidance Notes on Codes and Abbreviations" appearing at the beginning of each regular issue of the PCT Gazette.

Published:

— *with international search report*

PHOTONIC BAND-GAP OPTICAL FIBER WITH LARGE HOLLOW CORE

Technical Field

The present invention is in the field of optical waveguides and relates in particular to optical waveguides that guide light by virtue of a photonic bandgap.

Background Art

Optical fibre waveguides, which are able to guide light by virtue of a so-called photonic bandgap (PBG), were first proposed in 1995.

In, for example, "Full 2-D photonic bandgaps in silica/air structures", Birks et al., Electronics Letters, 26 October 1995, Vol. 31, No. 22, pp.1941-1942, it was proposed that a PBG may be created in an optical fibre by providing a dielectric cladding structure, which has a refractive index that varies periodically between high and low index regions, and a core defect in the cladding structure in the form of a hollow core. In the proposed cladding structure, periodicity was provided by an array of air holes that extended through a silica glass matrix material to provide a PBG structure through which certain wavelengths and propagation constants of light could not pass. It was proposed that light coupled into the hollow core defect would be unable to escape into the cladding due to the PBG and, thus, the light would remain localised in the core defect.

It was appreciated that light travelling through a hollow core defect, for example filled with air or even under vacuum, would suffer significantly less from undesirable effects, such as non-linearity and loss, compared with light travelling through a solid silica or doped silica fibre core. As such, it was appreciated that a PBG fibre may find application as a transmission fibre to transmit light over extremely long distances, for example across the Atlantic Ocean, without undergoing signal regeneration or as a high optical power delivery waveguide. In contrast, for standard index-guiding, single mode optical fibre, signal regeneration is typically required approximately every 80 kilometres.

The first hollow core PBG fibres that were attempted by the inventors had a periodic cladding structure formed by a triangular array of circular air holes embedded in a solid silica matrix and surrounding a central air core defect. Such fibres were formed by stacking circular or hexagonal capillary tubes, incorporating a core defect into the cladding by omitting a central capillary of the stack, and then heating and drawing the stack, in a one or two step process, to form a fibre having the required structure. The first fibres made by this process

had a core defect formed by the omission of a single capillary from the centre of the cladding structure.

US patent application US6404966 describes what is stated therein to be a PBG fibre having a hollow core region, which has an area of several times the optical wavelength, and a PBG cladding having a pitch equal to half the optical wavelength. The suggested advantage of the fibre is that it exhibits single mode behaviour.

International patent application PCT/GB00/01249 (The Secretary of State for Defence, UK), filed on 21 March 2000, proposed the first PBG fibre to have a so-called seven-cell core defect, surrounded by a cladding comprising a triangular array of air holes embedded in an all-silica matrix. The core defect was formed by omitting an inner capillary and, in addition, the six capillaries surrounding the inner capillary. This fibre structure appeared to guide one or two modes in the core defect, in contrast to the previous, single-cell core defect fibre, which appeared not to support any guided modes in the core defect.

According to PCT/GB00/01249, it appeared that the single-cell core defect fibre, by analogy to the density-of-states calculations in solid-state physics, would only support approximately 0.23 modes. That is, it was not surprising that the single-cell core defect fibre appeared to support no guided modes in its core defect. In contrast, based on the seven-fold increase in core defect area (increasing the core defect radius by a factor of $\sqrt{7}$), the seven-cell core defect fibre was predicted to support approximately 1.61 spatial modes in the core defect. This prediction was consistent with the finding that the seven-cell core defect fibre did indeed appear to support at least one guided mode in its core defect.

A preferred fibre in PCT/GB00/01249 was described as having a core defect diameter of around 15μm and an air-filling fraction (AFF) – that is, the proportion by volume of air in the cladding - of greater than 15% and, preferably, greater than 30%. Herein, AFF (or any equivalent measure for air or vacuum or other materials) is intended to mean the fraction by volume of air in a microstructured, or holey, portion of the cladding, which is representative of a substantially perfect and unbounded cladding. That is, imperfect regions of the cladding, for example near to or abutting a core defect and at an outer periphery of a microstructured region, would not be used in calculating the AFF. Likewise, a calculation of AFF does not take into account over-cladding or jacketing layers, which may surround the microstructured region.

In "Analysis of air-guiding photonic bandgap fibres", Optics Letters, Vol. 25, No. 2, January 15, 2000, Broeng et al. provided a theoretical analysis of PBG fibres. For a fibre with

a seven-cell core defect and a cladding comprising a triangular array of near-circular holes, providing an AFF of around 70%, the structure was shown to support one or two air guided modes in the core defect. This was in line with the finding in PCT/GB00/01249.

In the chapter entitled "Photonic Crystal Fibers: Effective Index and Band-Gap Guidance" from the book "Photonic Crystal and Light Localization in the 21st Century", C.M. Soukoulis (ed.), ©2001 Kluwer Academic Publishers, the authors presented further analysis of PBG fibres based primarily on a seven-cell core defect fibre. The optical fibre was fabricated by stacking and drawing hexagonal silica capillary tubes. The authors suggested that a core defect must be large enough to support at least one guided mode but that, as in conventional fibres, increasing the core defect size would lead to the appearance of higher order modes. This statement appears to contradict the position presented in the aforementioned US6404966, which prescribes a large core region and single mode behaviour. The authors of the chapter also went on to suggest that there are many parameters that can have a considerable influence on the performance of bandgap fibres: choice of cladding lattice, lattice spacing, index filling fraction, choice of materials, size and shape of core defect, and structural uniformity (both in-plane and along the axis of propagation).

WO 02/075392 (Corning, Inc.) identifies a general relationship in PBG fibres between the number of so–called surface modes that exist at the boundary between the cladding and core defect of a PBG fibre and the ratio of the radial size of the core defect and a pitch of the cladding structure, where pitch is the centre to centre spacing of nearest neighbour holes in the triangular array of the exemplified cladding structure. It is suggested that when the core defect boundary, together with the photonic bandgap crystal pitch, are such that surface modes are excited or supported, a large fraction of the "light power" propagated along the fibre is essentially not located in the core defect. Accordingly, while surface states exist, the suggestion was that the distribution of light power is not effective to realise the benefits associated with the low refractive index core defect of a PBG crystal optical waveguide. The mode energy fraction in the core defect of the PBG fibre was shown to vary with increasing ratio of core defect size to pitch. In other words, it was suggested that the way to increase mode energy fraction in the core defect is by decreasing the number of surface modes, in turn, by selecting an appropriate ratio of the radial size of the core defect and a pitch of the cladding structure. In particular, WO 02/075392 states that, for a circular core structure, a ratio of core radius to pitch of around 1.07 to 1.08 provides a high mode power fraction of not

less than 0.9 and is single mode. Other structures are considered, for example in Figure 7, wherein the core defect covers an area equivalent to 16 cladding holes.

In a Post-deadline paper presented at ECOC 2002, "Low Loss (13dB) Air core defect Photonic Bandgap Fibre", N. Venkataraman et al. reported a PBG fibre having a seven-cell core defect that exhibited loss as low as 13dB/km at 1500nm over a fibre length of one hundred metres. The structure of this fibre closely matches the structure considered in the book chapter referenced above. The authors attribute the relatively small loss of the fibre as being due to the high degree of structural uniformity along the length of the fibre.

PBG fibre structures are typically fabricated by first forming a pre-form and then heating and drawing an optical fibre from that pre-form in a fibre-drawing tower. It is known either to form a pre-form by stacking capillaries and fusing the capillaries into the appropriate configuration of pre-form, or to use extrusion.

For example, in PCT/GB00/01249, identified above, a seven-cell core defect pre-form structure was formed by omitting from a stack of capillaries an inner capillary and, in addition, the six capillaries surrounding the inner capillary. The capillaries around the core defect boundary in the stack were supported during formation of the pre-form by inserting truncated capillaries, which did not meet in the middle of the stack, at both ends of the capillary stack. The stack was then heated in order to fuse the capillaries together into a pre-form suitable for drawing into an optical fibre. Clearly, only the fibre drawn from the middle section of the stack, with the missing inner seven capillaries, was suitable for use as a hollow core defect fibre.

US patent application number US 6,444,133 (Corning, Inc.), describes a technique of forming a PBG fibre pre-form comprising a stack of hexagonal capillaries in which the inner capillary is missing, thus forming a core defect of the eventual PBG fibre structure that has flat inner surfaces. In contrast, the holes in the capillaries are circular. US 6,444,133 proposes that, by etching the entire pre-form, the flat surfaces of the core defect dissolve away more quickly than the curved surfaces of the outer capillaries. The effect of etching is that the edges of the capillaries that are next to the void fully dissolve, while the remaining capillaries simply experience an increase in hole-diameter. Overall, the resulting pre-form has a greater fraction of air in the cladding structure and a core defect that is closer to a seven-cell core defect than a single cell core defect.

PCT patent application number WO 02/084347 (Corning, Inc.) describes a method of making a pre-form comprising a stack of hexagonal capillaries of which the inner capillaries

are preferentially etched by exposure to an etching agent. Each capillary has a hexagonal outer boundary and a circular inner boundary, as illustrated in the diagram in Figure 11 herein. The result of the etching step is that the centres of the edges of the hexagonal capillaries around the central region dissolve more quickly than the corners, thereby causing formation of a core defect. In some embodiments, the circular holes are offset in the inner hexagonal capillaries of the stack so that each capillary has a wall that is thinner than its opposite wall. These capillaries are arranged in the stack so that their thinner walls point towards the centre of the structure. An etching step, in effect, preferentially etches the thinner walls first, thereby forming a seven-cell core defect.

Disclosure of the Invention

According to a first aspect, the present invention provides a photonic bandgap structure, having a plane cross section and a length dimension that extends perpendicular to the plane cross section, the photonic bandgap structure, in the plane cross section, comprising a substantially periodic array of relatively low refractive index regions, being separated from one another by relatively high refractive index regions, which extend along the photonic bandgap structure in the length dimension, the array having a characteristic primitive unit cell and a pitch Λ and comprising more than a seventy percent fraction by volume of relatively low refractive index regions; and

a core defect, surrounded by the photonic bandgap structure, the core defect comprising a region of relatively low refractive index having a plane cross section and a length dimension that extends perpendicular to the plane cross section, said plane cross section and length dimension being parallel to the same dimensions of the photonic bandgap structure, the area of the core defect region of relatively low refractive index being greater than sixteen times the area of the primitive unit cell. In other words, the area is greater than sixteen times the area of a single primitive unit cell, independently of shape or configuration.

Hitherto, the prior art teachings relating to PBG fibres have focused on a core defect that is just large enough to support a single mode, but not so large that it supports additional, unwanted modes. In practice, in the prior art, the preferred core defect size for fibres that have actually been made has generally been selected to be larger than a single unit cell but no larger than about the size of seven inner most capillaries, or unit cells, in a triangular array of capillaries. US patent application US6404966 purports to describe a single mode hollow core PBG fibre. However, it is unclear from the description how it would be possible to form a

single mode PBG fibre having a large hollow core defect, particularly if the cladding has a pitch which is only half the optical wavelength.

As will be described herein, the present inventors have demonstrated that increasing the core defect size beyond sizes proposed in the prior art teachings may provide significant benefits, which potentially outweigh the perceived or actual disadvantages of doing so.

The present inventors also demonstrate that at least some of the perceived disadvantages of increasing the core defect size, based on well-understood theory for index-guiding fibres, do not necessarily apply in the case of PBG fibres. In addition, the present inventors propose that, to the extent certain perceived disadvantages of increasing the core defect size do exist, there are ways to mitigate these effects by careful design of the PBG fibre structure. A number of possible ways to mitigate such effects will be considered. In particular, the inventors demonstrate that the number and kinds of modes that are supported by a PBG fibre are not determined only by the diameter of the core defect, an index difference between a core and cladding and wavelength of light, unlike in a conventional index-guiding fibre. Indeed, the present inventors demonstrate herein that it is possible to increase the diameter of the core defect significantly without proportionately increasing the numbers of core modes supported by the PBG fibre. In addition, the present inventors show that core modes supported by the PBG fibre can be manipulated by varying only the form of the boundary region around the core, as considered in more detail in applicant's co-pending patent application having the title "Optical Waveguide" (Ref. 0079WO) filed on the same date here as.

It is highly unlikely in practice that a photonic bandgap structure according to the present invention will comprise a 'perfectly' periodic array, due to imperfections being introduced into the structure during its manufacture and/or perturbations being introduced into the array by virtue of the presence of the core defect and/or additional layers (over-cladding) and jacketing around the photonic band-gap structure. The present invention is intended to encompass both perfect and imperfect structures. Likewise, any reference to "periodic", "lattice", or the like herein, imports the likelihood of imperfection.

As is well-known, a periodic, two-dimensional array, or lattice, can be defined by a primitive unit cell. A primitive unit cell is a unit cell of the structure, having a smallest area (in the transverse cross section) that, by vector translations, can tile and reproduce the entire structure without overlapping itself or leaving voids. The pitch Λ is the minimum translation distance between two neighbouring primitive unit cells.

A photonic bandgap structure as described herein typically has two-dimensional translational symmetry, in the plane cross-section, and is homogenous in the length direction. An exemplary primitive unit cell of a photonic bandgap structure can been seen in Figure 11, which illustrates a fibre preform comprising hexagonal capillaries 1105 arranged to form, on a macro-scale, a photonic bandgap structure around a core defect 1125. Referring to Figure 11, it can be seen that a single capillary 1105 can be tiled over the entire photonic bandgap structure, by translations in the x (or horizontal) direction, and translations at 30 degrees to the y (or vertical) direction. As such, a single capillary is an example of a primitive unit cell of the structure of Figure 11. Of course, the structure has an infinite number of other primitive unit cells, which have in common the same size and shape as a single capillary but are centred on a different part of the structure. For example, another primitive unit cell has its centre where a triangular arrangement of three neighbouring capillaries (e.g. point 1115) meet for the structure in Figure 11.

The term "primitive unit cell" is not used herein in its strict sense since, as already stated, a practical photonic bandgap structure is unlikely to be 'perfect' in form due to manufacturing imperfections and/or perturbations due to the presence of the core defect. Accordingly, a primitive unit cell of such a structure is likely to be at best only a close approximation to a primitive unit cell of an intended, perfect structure; and the term primitive unit cell is intended herein to cover such close approximations.

The core defect region of relatively low refractive index may be large enough to contain at least sixteen substantially whole primitive unit cells. In practical embodiments, the outer edges of one or more outer unit cells may be clipped or squeezed by the surrounding, imperfect structure, or by the introduction of a core boundary tube during manufacture (as described hereinafter). The potential for slight reductions of the size of one or more outer unit cells will be neglected for the purposes of defining what constitutes a whole primitive unit cell. In general, however, such an area should include sixteen whole primitive unit cells but, in addition, could include any number of partial primitive unit cells. Accordingly, the area could be the same as or larger than an area which is only sixteen times the area of a primitive unit cell, which could be made from either or both whole and partial primitive unit cells. The core defect region of relatively low refractive index may be substantially equal to nineteen times the area of the primitive unit cell. The core defect region of relatively low refractive index may be large enough to contain at least nineteen substantially whole primitive unit cells. In some embodiments, the area of the core defect region of relatively low refractive index

may be greater than thirty times the area of the primitive unit cell, for example it may hold around thirty seven primitive unit cells.

The core defect region of relatively low refractive index may have at least two-fold rotational symmetry. For example, the core region may be elongate, triangular, square, hexagonal, octagonal, dodecagonal or even circular. The core defect region may have six-fold rotational symmetry. Alternatively, the core defect may have no rotational symmetry or may be irregular or even random in form.

In preferred embodiments of the present invention, the relatively low refractive index regions of the photonic bandgap structure are arranged in an array, for example a triangular array. The primitive unit cell may be centred on a single relatively low refractive index region, that being the largest relatively low refractive index region in the primitive unit cell. In principle, a primitive unit cell may comprise various sizes of relatively low refractive index region, for example, as a result of interstitial holes forming between regions of relatively low index and relatively high index. In general, though, different sizes of low index and/or high index regions may be included within a primitive unit cell of the photonic bandgap structure.

The area of the core defect region of relatively low refractive index may be substantially equal to the area of a first primitive unit cell, a first group of all primitive unit cells that surround the first primitive unit cell and a second group of all primitive unit cells that surround said first group of primitive unit cells. In a triangular array, for example, the first group would comprise six primitive unit cells and the second group would comprise twelve primitive unit cells.

The core defect may have a form (for example approximate size, shape, configuration, topology, relationship with the photonic band-gap structure, etc.) that would be obtained by the omission or removal of relatively high refractive index regions from a first primitive unit cell, a first group of all primitive unit cells that surrounded the first primitive unit cell and a second group of all primitive unit cells that surrounded said first group of primitive unit cells. In some embodiments, omission or removal of that material would take place at the stage of forming a preform rather than during or after a fibre had been drawn from a preform. For example, where the primitive unit cells are glass capillaries, removal or omission of a relatively high index region would be equivalent to removing or omitting a capillary. However, for example, where relatively low index regions comprise a fluid (other than air) or a solid material, removal of relatively high index regions could be equivalent to replacing the those regions with additional relatively low index material. Even though such a

core defect may result from omission or removal of a fixed number of primitive unit cells, or respective relatively high index material, on a macro scale (for example in a preform), the area of the core defect in a final fibre structure may, on average, scale differently to the photonic bandgap structure as a result of the fabrication process. Accordingly, the core defect area in a final fibre structure may be, proportionately, larger or smaller than it was on the macro scale in the preform. For example, for a given number of missing or omitted primitive unit cells, significant variations in core defect diameter can result from pressurising the core defect to different pressures during a heating and drawing a preform step of production.

According to a second aspect, the present invention provides a photonic bandgap optical waveguide comprising:

a photonic bandgap structure, having a plane cross section and a length dimension that extends perpendicular to the plane cross section, the photonic bandgap structure, in the plane cross section, comprising a substantially periodic array of relatively low refractive index regions, being separated from one another by relatively high refractive index regions, which extend along the photonic bandgap structure in the length dimension, the array having a characteristic primitive unit cell and a pitch Λ, the primitive unit cell being centred on a single relatively low refractive index region, that being the largest relatively low refractive index region in the primitive unit cell; and

a core defect, surrounded by the photonic bandgap structure, the core defect comprising a region of relatively low refractive index having a plane cross section and a length dimension that extends perpendicular to the plane cross section, said plane cross section and length dimension being parallel to the same dimensions of the photonic bandgap structure, wherein the core defect has a form that would be obtained by the omission or removal of relatively high refractive index regions from a first primitive unit cell, a first group of all primitive unit cells that surrounded the first primitive unit cell and a second group of all primitive unit cells that surrounded said first group of primitive unit cells.

The photonic bandgap structure may comprise a substantially periodic, triangular array of relatively low refractive index regions. Then, the core defect may have a form that would be obtained by the omission or removal of relatively high refractive index regions from a first primitive unit cell, the six primitive unit cells that surround the first primitive unit cell and the twelve primitive unit cells that surround said six primitive unit cells. Other arrays, of course, may be used, for example, square, hexagonal or Kagome, to name just three.

In preferred embodiments of the present invention, the relatively low refractive index regions of the photonic bandgap structure are separated from one another by relatively high refractive index veins that are joined at nodes, each node having a diameter and each vein having a length and a thickness, at the mid-point along the length, and being joined at each end to a node.

Preferably, at least some of the nodes within the photonic bandgap structure have diameters that are significantly larger than the thickness of the veins that meet at the nodes. More preferably, substantially all of the nodes within the photonic bandgap structure have diameters that are significantly larger than the thickness of the veins that meet at the nodes.

Preferably, the nodes that are significantly larger than the thickness of the veins that meet at the nodes have a diameter that is at least 1.5 times the thickness of the veins. More preferably, the nodes that are significantly larger than the thickness of the veins that meet at the nodes have a diameter that is at least twice the thickness of the veins.

In preferred embodiments of the present invention the waveguide further comprises, in the plane cross section, a boundary at the interface between the core defect and the photonic bandgap structure, the boundary comprising a plurality of relatively high refractive index veins that are joined at nodes, each node having a diameter and each vein having a length and a thickness, at the mid-point along the length, and being joined at each end to a node.

Preferably, the fraction of nodes which have diameters that are significantly larger than the thickness of the veins that meet at the nodes is less on the boundary than in a similar region of the photonic bandgap structure. For example, the boundary may include substantially no nodes which have diameters that are significantly larger than the thickness of the veins that meet at the nodes.

Some embodiments may further comprise, in the plane cross section, a boundary at the interface between the core defect and the photonic bandgap structure, the boundary comprising a plurality of relatively high refractive index boundary veins joined end-to-end around the boundary between boundary nodes, each boundary vein having a length l and a thickness t, at the mid-point along the length l, and being joined between a leading boundary node and a following boundary node, and each boundary node having a diameter and being joined between two boundary veins and to a relatively high refractive index region of the photonic bandgap structure, wherein, in the plane cross section, around the boundary:

$t < d_L$ and $t < d_F$ is true for more than half of the boundary veins; and

$l \geq x(d_L+d_F)$ is true for at least one boundary vein,

where $x \geq 0.6$ and d_L, d_F are the diameters of the leading and following nodes respectively for each vein.

The present inventors have found that core boundaries having the aforementioned (and respective following) particular length and diameter relationships also find general application in waveguides having smaller core regions than in accord with the present invention. For example, such boundaries provide benefits even in the seven cell core defect structures S2 and S3 as shown in Figure 3, and even smaller core defects, for example of three cell design. Indeed, such core boundaries are not limited in their use by core area, as long as there are sufficient nodes and veins.

In addition, core boundaries having the aforementioned (and respective following) particular length and diameter relationships may be used in combination with periodic or non-periodic photonic band-gap structures. Although periodic arrays are more common for forming a photonic band-gap, in principle, the array need not be periodic – see, for example, "Antiresonant reflecting photonic crystal optical waveguides", by N. M. Litchinitser et al., Optics Letters, Volume 27, No. 18, September 15, 2002, pp1592-1594. Although this paper does not provide calculations explicitly for PBG fibres, it does illustrate that photonic bandgaps may be obtained without periodicity.

The diameter of a node may be measured as the diameter of the largest inscribed circle that fits within the region that makes up the node. The length of a vein may be measured along the centre-line of the vein between said largest circles that fit within the nodes at either end of the vein.

Length $l \geq x(d_L+d_F)$ may be true for a plurality of the boundary veins, at least half of the boundary veins or, even, for all of the boundary veins.

The waveguide may be arranged so that $x \geq 0.8$. The waveguide may be arranged so that $x \geq 1.0$. In some embodiments, the waveguide may be arranged so that $x \geq 1.5$, 2.0, 2.5 or even 3.0.

In the plane cross section, the thinnest point along at least some of the boundary veins may be substantially at the mid-point. For example, a vein may be relatively thick at one end, taper down towards a minimum thickness at the mid-point and then thicken back up towards the other end. In some embodiments, each boundary vein has a thinnest point substantially at the midpoint. Alternatively, at least some veins may have a relatively thicker portion at or near the mid-point. For example, a vein may be relatively thick at one end, taper down and thicken back up to a local maximum thickness at the mid-point, which is less than the

thickness at the first-mentioned end, and then taper down and thicken back up again towards the other end.

Given an array with a pitch Λ, it is possible to relate the thickness of the boundary veins to a pitch of the photonic bandgap structure. For example, the thickness at the midpoint of a plurality of the boundary veins, or in some embodiments substantially all of the boundary veins, may be less than 0.1Λ. In some embodiments, the thickness at the mid-point of a plurality of the boundary veins, or in some embodiments substantially all of the boundary veins, is less than 0.049Λ.

At least some boundary nodes may have diameters that are significantly smaller than at least some nodes in the photonic bandgap structure. In some embodiments, substantially all boundary nodes have diameters that are significantly smaller than at least some nodes, or even a significant proportion of all nodes, in the photonic bandgap structure.

The diameters of at least some of the nodes within the photonic bandgap structure, or even a significant proportion of all, or all, nodes within the photonic bandgap structure, may be significantly larger than the mid-point thickness of the veins that are joined to the respective nodes.

In preferred embodiments of the present invention, at least some of the relatively low refractive index regions are voids filled with air or under vacuum. Additionally or alternatively, at least some of the relatively low refractive index regions are voids filled with a gas other than air or a liquid.

Additionally, or alternatively, at least some of the relatively high refractive index regions comprise silica glass. As used herein 'silica' encompasses fused silica, including doped fused silica, and silicate glasses in general such as germano-silicates and boro-silicates.

In alternative embodiments of the invention the region may be a material other than silica. For example, it may be another inorganic glass or an organic polymer.

At least some of the boundary veins may be substantially straight. Indeed, all of the boundary veins may be straight. Alternatively, at least some of the boundary veins may be bowed outwardly from the core defect, or inwardly into the core defect, between their respective nodes.

Preferably, the waveguide has a proportion by volume of relatively low refractive index regions that is greater than 75%. The proportion may be greater than 80%, greater than 85%, greater than 90% or even greater than 92%. We have found particularly wide photonic bandgaps at proportions by volume of relatively low refractive index region exceeding 90%.

According to preferred embodiments of the present invention, the waveguide supports a mode in which greater than 95% of the mode power in the waveguide is in relatively low refractive index regions. Preferably, the relatively low refractive index regions comprise air or are under a vacuum. More preferably, the waveguide supports a mode in which greater than 98% of the mode power in the waveguide is in relatively low refractive index regions. Even more preferably, the waveguide supports a mode in which greater than 99%, or even greater than 99.9%, of the mode power in the waveguide is in air.

Preferably, the waveguide supports a mode having a mode profile that closely resembles the fundamental mode of a standard, single mode optical fibre. Additionally, said mode preferably supports a maximum amount of the mode power in relatively low refractive index regions compared with other modes that are supported by the waveguide.

The waveguide may support a core-guided, non-degenerate mode, for example a mode resembling a TE_{01} mode or a TM_{01} mode. Indeed, the present inventors have found that these kinds of modes exist in a large sample of different structures, whether those structures are in accord with the present invention or not. For example, the non-degenerate modes occur in structures having smaller core regions as well. These modes typically occur at slightly shorter wavelengths than the typical fundamental-type modes.

The waveguide may support plural core-guided (for example, air-guided) modes.

The waveguide may have an operating wavelength, wherein the pitch Λ of the photonic band-gap structure is greater than the operating wavelength. Typically, the pitch is greater than 1.5 times the operating wavelength. According to embodiments presented herein, the pitch is more than twice the operating wavelength. (It should be noted that there are many parameters, such the filling fraction of the relatively low refractive index regions (e.g. air) and pitch, that can be altered when designing a photonic band-gap structure. Different combinations of values of those parameters may produce, for example, bandgaps over the same or very similar wavelength ranges. Accordingly, we provide herein various lists of parameter values. It should be understood that all functioning combinations of those (or different) values are within the scope of the invention, except where context, sense, or the limits of physical possibility dictate otherwise.)

According to a third aspect, the present invention provides an optical fibre comprising a waveguide as described above. In preferred embodiments, the optical fibre has a transmission loss of less than 12dB/km.

According to a fourth aspect, the present invention provides a transmission line for carrying data between a transmitter and a receiver, the transmission line including along at least part of its length the fibre according to the third aspect.

According to a fifth aspect, the present invention provides a preform for making a photonic bandgap optical waveguide, the preform comprising:

a first part for forming a photonic bandgap structure of the photonic bandgap optical waveguide, the first part having a plane cross section and a length dimension that extends perpendicular to the plane cross section and, in the plane cross section, a substantially periodic array of relatively low refractive index regions, being separated from one another by relatively high refractive index regions, which extend along the first part in the length dimension, the array having a characteristic primitive unit cell and a pitch; and

a relatively low-index region which becomes a core defect in the photonic bandgap structure of the photonic bandgap optical waveguide, the relatively low index region being surrounded by said first part and having a plane cross section and a length dimension that extends perpendicular to the plane cross section, said plane cross section and length dimension being parallel to the same dimensions of said first part, the area of the relatively low index region being greater than sixteen times the area of the primitive unit cell.

According to a sixth aspect, the present invention provides a preform for making a photonic bandgap optical waveguide, the preform comprising:

a first part for forming a photonic bandgap structure of the photonic bandgap optical waveguide, the first part having a plane cross section and a length dimension that extends perpendicular to the plane cross section and, in the plane cross section, a substantially periodic array of relatively low refractive index regions, being separated from one another by relatively high refractive index regions, which extend along the first part in the length dimension, the array having a characteristic primitive unit cell and a pitch, the primitive unit cell being centred on a single relatively low refractive index region and encompassing no more than one relatively low refractive index region; and

a relatively low-index region which becomes a core defect in the photonic bandgap structure of the photonic bandgap optical waveguide, the relatively low index region being surrounded by said first part and having a plane cross section and a length dimension that extends perpendicular to the plane cross section, said plane cross section and length dimension being parallel to the same dimensions of said first part, the core defect has a form that would be obtained by the omission or removal of relatively high refractive index regions

from a first primitive unit cell, a first group of all primitive unit cells that surround the first primitive unit cell and a second group of primitive unit cells that surround said first group of primitive unit cells.

According to a seventh aspect, the present invention provides a method of forming a photonic bandgap optical waveguide by forming the aforementioned preform, which is described as being in accord with the present invention, and heating and drawing the preform into a photonic bandgap optical waveguide. The waveguide may comprise a PBG fibre and, then, the PBG fibre may have a transmission loss less than 12dB/km.

According to a eighth aspect, the present invention provides a method of forming a photonic bandgap optical waveguide comprising the steps:

forming a preform stack by stacking a plurality of elongate elements into a periodic, triangular array of elements, the elongate elements comprising a relatively low refractive index elongate inner region enclosed by a relatively high refractive index outer region;

omitting, or substantially removing from an inner region of the stack, a first element, a first number comprising all elements from around said first element and a second number comprising all elements from around said first number of elements; and

heating and drawing the stack, in one or more steps, into a photonic bandgap optical waveguide, characterised by a photonic bandgap structure that surrounds a core defect, the photonic bandgap structure having a plane cross section and a length dimension that extends perpendicular to the plane cross section and comprising, in the plane cross section, a periodic, triangular array of relatively low refractive index regions, being separated from one another by relatively high refractive index regions, which extend along the photonic bandgap structure in the length dimension.

The preform stack may comprise a substantially periodic, triangular array of elongate elements. Then, the inner region of the stack may be formed by omission or substantial removal of a first element, the six elements that surround the first elements and the twelve elements that surround said six elements.

The elements may have a generally hexagonal transverse cross section or a generally circular transverse cross section.

For example, for generally circular cross section elements, first elongate interstitial voids are formed between elements.

The method may include the additional step of introducing further elongate elements into at least some of the first interstitial voids. At least some of the further elongate elements

may comprise rods. Additionally, or alternatively, at least some of the further elongate elements may comprise capillaries. Use of capillaries provides the option to control more closely the volume of glass that is added to an interstitial void for a given outer diameter of capillary. The further elongate elements may be introduced into substantially all of the first interstitial voids.

The method may comprise the additional step of introducing an inner elongate element into the inner region to support the elements around the inner region. As such, second interstitial voids may be formed between the elements around the inner region and the inner elongate element and the method may include the step of introducing additional elongate elements into at least some of the second interstitial voids. Again, at least some of the additional elongate elements may comprise rods. Additionally or alternatively at least some of the additional elongate elements may comprise capillaries.

A reduced fraction of the additional elements may be introduced into the second interstitial voids compared with the number of elements that are introduced into a similar configuration of first interstitial voids. In some embodiments, no additional elongate elements are introduced into the second interstitial voids.

Alternatively, at least some of the additional elongate elements that are introduced into the second interstitial voids may have a smaller cross sectional area than the elongate elements that are introduced into the first interstitial voids.

In preferred embodiments of the present invention, the inner elongate element has a relatively low refractive index elongate inner region enclosed by a relatively high refractive index outer region, which becomes part of the photonic bandgap optical waveguide. The inner elongate element may comprise a capillary tube.

Alternatively, the inner elongate element may comprise a material that has a higher coefficient of thermal expansion than the relatively high refractive index material in the elongate elements. Accordingly, the method may comprise the further steps of:

heating the preform stack in order to fuse the elongate elements around the further elongate element;

cooling the preform stack; and

removing the inner elongate element from the preform stack prior to heating and drawing the preform stack.

Preferably, at least some of the relatively low refractive index regions comprise air or are under vacuum. Alternatively, at least some of the relatively low refractive index regions

are voids filled with a gas other than air or a liquid. Additionally, or alternatively, at least some of the relatively high refractive index regions may comprise silica glass, although they could comprise a different inorganic glass or even an organic polymer.

According to a ninth aspect, the present invention provides an optical fibre comprising a photonic bandgap optical waveguide made by the above-described method. The optical fibre preferably has a transmission loss below 12dB/km.

According to a tenth aspect, the present invention provides an optical waveguide, having a plane cross section and a length dimension, which extends perpendicular to the plane cross section, comprising:

a photonic bandgap structure for providing a photonic bandgap over a range of frequencies of light, the photonic bandgap structure comprising, in the plane cross section, an arrangement of relatively low refractive index regions interspersed with relatively high refractive index regions, which extend parallel to the length dimension;

a core defect comprising a region of relatively low refractive index, which extends parallel to the length dimension and through the photonic bandgap structure; and

a boundary at the interface between the core defect and the photonic bandgap structure, the boundary, in the plane cross section, comprising a plurality of relatively high refractive index boundary veins joined end-to-end around the boundary between boundary nodes, each boundary vein having a length l and a thickness t, at the mid-point along the length l, and being joined between a leading boundary node and a following boundary node, and each boundary node having a diameter and being joined between two boundary veins and to a relatively high refractive index region of the photonic bandgap structure, wherein, in the plane cross section, around the boundary:

$t < d_L$ and $t < d_F$ is true for more than half of the boundary veins; and

$l \geq x(d_L+d_F)$ is true for at least one boundary vein,

where $x \geq 0.6$ and d_L, d_F are the diameters of the leading and following nodes respectively for each vein.

According to an eleventh aspect, the present invention provides a method of forming a photonic bandgap optical waveguide having a plane cross section and a length dimension, which extends perpendicular to the plane cross section, comprising the steps:

forming a preform stack by stacking a plurality of elongate elements;

omitting, or substantially removing at least one elongate element from an inner region of the stack; and

heating and drawing the stack, in one or more steps, into a photonic bandgap optical waveguide,

characterised by a photonic bandgap structure, a core defect and a boundary at the interface between the core defect and the photonic bandgap structure,

the photonic bandgap structure for providing a photonic bandgap over a range of frequencies of light, the photonic bandgap structure comprising, in the plane cross section, an arrangement of relatively low refractive index regions interspersed with relatively high refractive index regions, which extend parallel to the length dimension,

the core defect comprising a region of relatively low refractive index, which extends parallel to the length dimension and through the photonic bandgap structure,

the boundary at the interface between the core defect and the photonic bandgap structure, the boundary, in the plane cross section, comprising a plurality of relatively high refractive index boundary veins joined end-to-end around the boundary between boundary nodes, each boundary vein having a length l and a thickness t, at the mid-point along the length l, and being joined between a leading boundary node and a following boundary node, and each boundary node having a diameter and being joined between two boundary veins and to a relatively high refractive index region of the photonic bandgap structure, wherein, in the plane cross section, around the boundary:

$t < d_L$ and $t < d_F$ is true for more than half of the boundary veins; and

$l \geq x(d_L+d_F)$ is true for at least one boundary vein,

where $x \geq 2$ and d_L, d_F are the diameters of the leading and following nodes respectively for each vein.

Brief Description of the Drawings

Embodiments of the present invention will now be described, by way of example only, with reference to the accompanying drawings, of which:

Figure 1 is a diagram of a transverse cross section of a PBG fibre structure of the kind known from the prior art;

Figure 2 is a diagram which illustrates how various physical characteristics of PBG fibres are defined herein;

Figures 3 and 4 show diagrams of various examples of PBG fibre structures;

Figures 5 and 6 show mode spectra plots for the PBG fibre structures of Figures 3 and 4;

Figure 7 shows mode intensity distribution plots for a mode, supported by each structure of Figures 3 and 4, which supports the highest amount of light in air;

Figures 8 and 9 show graphs of mode intensity for x and y axes of the distributions of Figure 7;

Figure 10 is a mode intensity distribution plot for a mode, supported by an alternative structure, which supports the highest amount of light in air;

Figure 11 is a diagram of a pre-form suitable for making PBG fibre according to the prior art;

Figure 12 is a diagram of a pre-form suitable for making a fibre according to examples of PBG fibres described hereinafter;

Figure 13 shows scanning electron micrograph (SEM) images of seven cell core defect fibres made using a preform of the kind illustrated in Figure 12;

Figure 14 is a diagram of an alternative pre-form suitable for making a fibre according to embodiments of the present invention;

Figure 15 shows an SEM image of a nineteen cell core defect fibre made using a preform of the kind illustrated in Figure 14; and

Figure 16 shown a loss graph for the fibre represented in the image of Figure 15.

Figure 17 is a diagram of a further alternative pre-form suitable for making a fibre according to embodiments of the present invention;

Figure 18 is a diagram of a further alternative pre-form suitable for making a fibre according to embodiments of the present invention;

Figure 19 is a diagram of a further alternative pre-form suitable for making a fibre according to embodiments of the present invention; and

Figure 20 is a diagram of an outer region of a preform stack according to embodiments of the present invention, wherein the stack is contained in a large, thick-walled capillary and interstitial regions between the inner surface of the large, thick-walled capillary and the stack contain various sizes of solid packing rod.

Best Mode For Carrying Out the Invention, & Industrial Applicability

Figure 1 is a representation of a transverse cross-section of a fibre structure of the kind described in the prior art and is used herein as a reference against which the characteristics of other structures described herein are compared. In the Figure, the black regions represent fused silica glass and the white regions represent air holes in the glass. As illustrated, the

cladding 100 comprises a triangular array of generally hexagonal cells 105, surrounding a seven-cell core defect 110. A core defect boundary 145 is at the interface between the cladding and the core defect. The core defect boundary has twelve sides – alternating between six relatively longer sides and six relatively shorter sides - and is formed by omitting or removing seven central cells; an inner cell and the six cells that surround the inner cell. The cells would have typically been removed or omitted from a pre-form prior to drawing the pre-form into the fibre. As the skilled person will appreciate, although a cell comprises a void, or a hole, for example filled with air or under vacuum, the voids or holes may alternatively be filled with a gas or a liquid or may instead comprise a solid material that has a different refractive index than the material that surrounds the hole. Equally, the silica glass may be doped or replaced by a different inorganic glass or other suitable material such as an organic polymer.

Two longitudinal planes through the fibre structure of Figure 1 are denoted y and x; with y being a vertical plane passing through the centre of the structure and x being a horizontal plane passing through the centre of the structure as shown.

Hereafter, and with reference to Figure 1, a region of glass 115 between any two holes is referred to as a "**vein**" and a region of glass 120 where veins meet is referred to as a "**node**".

The core defect boundary 145 comprises the inwardly-facing veins of the innermost ring of cells that surround the core defect 110.

In practice, for triangular array structures that have a large air-filling fraction, for example above 75%, most of the cladding holes 105 assume a generally hexagonal form, as shown in Figure 1, and the veins are generally straight.

Figures 2a and 2b are diagrams which illustrate how various dimensions of the cladding structure of Figure 1 are defined herein, with reference to four exemplary cladding cells 200.

For the present purposes, a node 210' in the cladding, which is referred to herein as a "**cladding node**", is said to have a diameter measurement **d** defined by the largest diameter of inscribed circle that can fit within the glass that forms the node. A vein 205 in the cladding, which is referred to herein as a "**cladding vein**", has a length **l**, measured along its centre-line between the circles of the cladding nodes 210 & 210' to which the cladding vein is joined and a thickness, **t**, measured at its mid-point between the respective cladding nodes. Generally, herein, veins increase in thickness towards the nodes to which they are joined.

The mid-point of a cladding vein is typically the thinnest point along the vein. Unless otherwise stated herein, generally, a specified vein thickness is measured at the mid-point of the vein between the two nodes to which the vein is joined.

According to Figure 2, a cladding node is surrounded by three notional circular paths 215, each one being positioned between and abutting a different pair of neighbouring cladding veins that join the node. These three paths, in effect, define the 'roundness' of the corners of the cladding holes and abut the notional inscribed circle that defines the diameter of the respective node. More particularly, the periphery of the node between each pair of veins is defined by the portions of the circular paths 215 which begin at a point p and end at a point q along first and second veins respectively. Points p and q are equidistant from the centre of the node 210'. It will be appreciated that the diameter, d, of the node 210' is a function of the thickness, t, of the veins, the distance of p from the centre of the node and the pitch Λ, or centre to centre distance between neighbouring cells, of the structure.

The cells forming the innermost ring around the boundary of the core defect, which are referred to herein as "**boundary cells**", have one of two general shapes. A first kind of boundary cell 125 is generally hexagonal and has an innermost vein 130 that forms a relatively shorter side of the core defect boundary 145. A second kind of boundary cell 135 has a generally pentagonal form and has an innermost vein 140 that forms a relatively longer side of the core defect boundary 145.

There are twelve boundary cells 125, 135 and twelve nodes 150, which are referred to herein as "**boundary nodes**", around the core defect boundary 145. Specifically, as defined herein, there is a boundary node 150 wherever a vein between two neighbouring boundary cells meets the core defect boundary 145. In Figure 1, these boundary nodes 150 have slightly smaller diameters than the cladding nodes 160. Additionally, there is an enlarged region 165, or "**bead**", of silica at the mid point of each relatively longer side of the core defect boundary 145. These beads 165 coincide with the mid-point along the inner-facing vein 140 of each pentagonal boundary cell 135. The beads 165 may result from a possible manufacturing process used to form the structure in Figure 1, as will be described in more detail below. For the present purposes, the veins 130 & 140 that make up the core defect boundary are known as "**boundary veins**".

As will be described below, it is possible to control the diameters of particular nodes and the existence or size of beads along the core defect boundary during manufacture of a fibre.

The structure in Figure 1 and each of the following examples of different structures closely resemble practical optical fibre structures, which have either been made or may be made according to known processes or the processes described hereinafter. The structures share the following common characteristics:

a pitch Λ of the cladding chosen between values of approximately 3μm and 6μm (this value may be chosen to position core-guided modes at an appropriate wavelength for a particular application);

a thickness t of the cladding veins of 0.0586 times the chosen pitch Λ of the cladding structure (or simply 0.0586Λ);

an AFF in the cladding of approximately 87.5%; and

a ratio **R** having a value of about 0.5.

Referring to Figure 2, **R** is defined as the ratio of the distance of p' from the centre of the nearest cladding node to half the length of a cladding vein, **l/2**; where p' is a point along the centre-line of a cladding vein and is defined by a construction line that passes through the centre-line of the vein, the centre of circle 215 and the point p where the circle meets the vein.

In effect, R is a measure of the radius of curvature of the corners of the hexagonal cells within the cladding. It will be apparent that the maximum practical value of R is 1, at which value the radius of curvature is a maximum and the cladding holes are circular. The minimum value of R is dictated by the thickness t and length l of the veins and is the value at which the diameter of the circle 215 tends to zero and the cladding holes are hexagonal.

For all values of R below the maximum value, the veins appear to have a region of generally constant thickness about their mid-points, which increases in length with decreasing R. For example, a value of R=0.5 provides that around half the length of a vein, about its mid-point, has a substantially constant thickness. Likewise, a value of R=0.25 provides that around three quarters of the length of a vein, about its mid-point, has a substantially fixed thickness.

Given R, t and Λ, for practical purposes, the diameter d of the cladding nodes is found to be approximately:

$$d = \frac{2R\Lambda}{\sqrt{3}} - \Lambda R + t \qquad \text{(Equation 1)}$$

In Figure 1, the diameter of each boundary node 150, d_c, is smaller than the diameter of the cladding nodes 160, due to there being less glass available at the boundary for forming the nodes. A model similar to that shown in Figure 2 may if required be used to define the form of the boundary nodes. The differences between Figure 2 and the model for the boundary nodes are (1) the boundary node model includes the core defect 110 and two boundary cells rather than three cladding cells, (2) it is assumed that the value of R is a minimum, such that there is no measurable circular path inside the core defect 110; and, (3) the internal angles of the core defect and the boundary cells are different from each other and from the cells in the cladding.

The beads 165 shown in Figure 1 are substantially oval shaped, each having a major dimension which is approximately 1/3 the length of the distance between the two node centres that lie on either side of the bead and a minor dimension which is 1/3 the length of the major dimension. The minor dimension of the bead, which defines the thickness of the associated vein at its mid-point, is slightly longer than the diameter of the respective boundary nodes 150.

For boundary veins with no beads, the thickness at the mid-point of the vein between boundary nodes is the same as the thickness of the cladding veins at the same point.

The present inventors have determined that it is possible to control the performance of PBG fibres in particular by aiming to maximise the amount of light that propagates in air within the fibre structure, even if some light is not in the core, in order to benefit from the properties of PBG fibres, such as reduced absorption, non-linearity and, in addition, reduced mode coupling.

For the purposes of comparing aspects of the performance of various different structures it is useful to consider the modes that are supported in the band gap of various PBG fibre structures. This may be achieved by solving Maxwell's vector wave equation for the fibre structures, using known techniques. In brief, Maxwell's equations are recast in wave equation form and solved in a plane wave basis set using a variational scheme. An outline of the method may be found in Chapter 2 of the book "Photonic Crystals – Molding the Flow of Light", J.D. Joannopoulos et al., ©1995 Princeton University Press.

Figures 3 and 4 illustrate six exemplary PBG fibre structures that will be considered hereafter. Figure 3 illustrates three structures identified as S1, S2 and S3 herein, which are seven-cell core defect structures. S1 is the same as the structure illustrated in Figure 1 and is reproduced in Figure 3 for convenience only. S2 and S3, while not being embodiments of the

present invention per se, reinforce various characteristics of the invention, as determined by the present inventors, and, in particular, are discussed herein in order to illustrate how the mode spectrum of a given structure may vary significantly, compared with S1, without varying the size of the core defect but, instead, varying different core defect boundary characteristics.

Figure 4 illustrates three structures identified as S4, S5 and S6, which are exemplary embodiments of the present invention, each having a nineteen-cell core defect. S4, S5 and S6, apart from core defect size, have the same cladding characteristics as S1, S2 and S3 respectively. S1 to S3 have a maximum core defect radius of about 1.5Λ. In contrast, S4 to S6 have a maximum core defect radius of about 2.5Λ.

The characteristics of structures S2 to S6 will now be described in further detail.

There are a number of differences between the form of the core defect boundary in S1 and the boundary in S2. S2 has reduced boundary node diameters, which are significantly smaller than the cladding nodes 360, compared with S1, and no apparent beads along the core defect boundary 345. According to the definitions provided herein, the boundary nodes 355 in S2 have a minimum diameter; the associated values of R are at a minimum and, accordingly, there are no measurable circular paths defining the periphery of the nodes. The diameters of the boundary nodes 355 in S2 are only very slightly larger than the thickness of the boundary veins 330, 340. In contrast, as for S1, the cladding nodes 360 have diameters that are significantly larger than the thickness of their adjoining veins 315.

It may in practice be difficult to make the exact structure of S2 due to surface tension effects acting on the glass during the drawing process, which may cause the cladding veins to meet the boundary veins at slightly rounded corners; meaning R is not its theoretical minimum. However, it is useful to compare the characteristics of S2 with the other structures herein. Structures closely resembling S2, however, can be made according to a method that will be described in detail below.

The boundary in S3 has no apparent beads, as in S2, and the boundary nodes 355 have a similar diameter to those in S1.

The structure in S4 has an additional ring of cladding cells removed from around the core defect compared with S1. This forms a core defect 410 equivalent to nineteen missing cladding cells. Similar to S1, S4 has boundary nodes 450 that are significantly larger in diameter than the thickness of the respective boundary veins and there are hexagonal cells 425 at each corner of the core defect 410. However, in contrast to S1, which has one generally

pentagonal cell along each side of the core defect boundary 145, S4 has two generally pentagonal cells 435 along each side of the core defect boundary 445. In addition, there are two beads 455 along each side of the core defect boundary 445, roughly coincident with the mid-point of the vein 440 of each pentagonal cell 425 that borders the core defect boundary 445. The minor dimension of each bead is slightly longer than the diameter of the nodes to which each respective vein is joined. There are also three boundary nodes 455 per relatively longer side of the core defect boundary 445, compared with two for the seven-cell core defect structures. Overall, S4 has eighteen cells sharing veins with the core defect boundary 445. S4 represents an exemplary embodiment of the present invention.

The boundary in S5 is similar to S2 in the respect that it has reduced-diameter boundary nodes 455', which do not have diameters that are significantly larger than the thickness of the respective veins, and there are no apparent beads. All other parameters of S5 are the same as S4. S5 represents an exemplary embodiment of the present invention.

The boundary in S6 has no apparent beads, as in S3, and the boundary nodes 455 have a similar diameter to those in S1. All other parameters of S6 are the same as S4. S6 represents an exemplary embodiment of the present invention.

Figures 5 and 6 each show three mode spectra, identified as P1 to P3 and P4 to P6 respectively. Each spectrum P1 to P6 relates to a respective PBG fibre structure S1 to S6. The horizontal axis of each spectrum is normalised frequency, $\omega\Lambda/c$, where ω is the frequency of the light, Λ is the pitch of the cladding structure, and c is the speed of light in a vacuum. The vertical axis of each spectrum relates to the response of the structure to a given input for a given normalised wave-vector $\beta\Lambda=13$, against which the spectrum is plotted, where β is the chosen propagation constant for the calculations. The spectra are produced using a Finite-difference Time Domain (FDTD) algorithm, which computes the time-dependent response of a given hollow core structure to a given input. This technique has been extensively used in the field of computational electrodynamics, and is described in detail in the book "Computational Electrodynamics: The Finite-Difference Time-Domain Method", A. Taflove & S.C. Hagness, ©2000 Artech House. The FDTD technique may be readily applied to the field of PBG fibres and waveguides by those skilled in the art of optical fibre modelling.

With reference to spectra P1 to P6, each vertical spike indicates the presence of at least one mode at a corresponding normalised frequency. In some cases, multiple modes may appear as a single spike or as a relatively thicker spike compared with other spikes in a spectrum. This is due to the fact that the data used to generate the spectra is not of a high

enough resolution to distinguish very closely spaced modes. As such, the mode spectra should be taken to provide only an approximation to the actual numbers of modes that exist for each structure, which is satisfactory for enabling a general comparison between spectra herein.

On each spectrum, a 'light line' for the respective structure is shown as a solid vertical line at $\omega\Lambda/c=13=\beta\Lambda$, and band edges, which bound a bandgap, are represented as two dotted vertical lines, one on either side of the light line, with a lower band edge of the bandgap at around $\omega\Lambda/c=12.92$ and an upper band edge of the bandgap at around $\omega\Lambda/c=13.30$. A bandgap in P1 to P6 is a range of frequencies of light for a given β. For the present examples, the bandgap is slightly wider than 0.35 (in units of $\omega\Lambda/c$). The inventors estimate that the minimum practical width for a PBG fibre bandgap would be around 0.05 in the present units of measure but, more preferably, would be greater than 0.1.

Modes that are between the light line and the lower band edge (that is, to the left of the light line) will concentrate in the glass and be evanescent in air whereas the modes that are between the light line and the upper band edge (that is, to the right of the light line) may be air-guiding.

As shown in P1, relating to S1, there are around three modes between the light line and the lower band edge and around nine modes between the light line and the upper band edge (taking the thicker spikes as two modes). It is clear that S1 supports a significant number of modes, some of which could be air-guiding; although, it is unlikely that all of these modes will be excited by a given light input. Analysis of the individual modes shown in the bandgap of P1 leads to a finding that the mode marked as F1 is an air-guiding mode, which most closely resembles the form of a fundamental mode in a typical standard optical fibre and supports the maximum amount of light in air. The mode is found to be degenerate, being one of a pair of very similar modes falling at about the same position in the bandgap.

As shown in P2, relating to S2, approximately two modes lie between the light line and the lower band edge and there are around twelve modes between the light line and the upper band edge. As with S1, S2 supports a significant number of modes, some of which could be air-guiding. The mode marked F2 in P2 is found to be a degenerate, air-guiding mode that most closely resembles the form of a fundamental mode in a typical standard optical fibre and supports the maximum amount of light in air.

The structural characteristics of S2 are not that different from those of S1; the only differences being the reduced boundary node sizes in S2 and omission of the beads. Notably,

the core defect diameters of the two structures are the same. However, the mode spectra for the two structures are significantly different, there being more potentially-air-guiding modes supported by S2 but fewer modes that are evanescent in air.

As shown in P3, relating to S3, there are around three modes between the light line and the lower band edge and around thirteen modes between the light line and the upper band edge. Again, it is clear that S3 supports a significant number of modes, some of which could be air-guiding. The mode marked F3 in P3 is a degenerate, air-guiding mode that most closely resembles the form of a fundamental mode in a typical standard optical fibre and supports the maximum amount of light in air.

Again, the structural characteristics of S3 are only subtly different from those of either S1 or S2, with the core defect diameters of all structures being the same. However, the mode spectrum for S3 is, once more, significantly different from the mode spectra of either S1 or S2.

As shown in P4, relating to S4, which is a nineteen-cell core defect structure, there are approximately two to four modes between the light line and the lower band edge and in excess of twenty modes between the light line and the upper band edge of the bandgap region. Clearly, S4 appears to support significantly more modes than any of the foregoing seven-cell core defect structures. The mode marked F4 in P4 is again a degenerate, air-guiding mode that most closely resembles the form of a fundamental mode in a typical standard optical fibre and supports the maximum amount of light in air.

The core defect diameter of S4 is significantly larger than in S1, whereas the other parameters are substantially the same. On the basis of prior art thinking it is not a surprise that there appear to be significantly more modes supported in the nineteen-cell core defect structure of S4 than in any of the seven-cell core defect structures S1 to S3.

As shown in P5, relating to S5, there are approximately four modes between the light line and the lower band edge and around fifteen to twenty modes between the light line and the upper band edge. Again, S5 appears to support significantly more modes than the foregoing seven-cell core defect structures. The mode marked F5 in P5 is a degenerate, air-guiding mode that most closely resembles the form of a fundamental mode in a typical standard optical fibre and supports the maximum amount of light in air.

The mode spectra for S4 and S5 are similar in terms of numbers of modes, with both structures supporting a number of evanescent and possibly air-guiding modes.

As shown in P6, relating to S6, there is a single mode between the light line and the lower band edge and approximately twelve to fifteen modes between the light line and the upper band edge. Thus, S6 appears to support significantly fewer modes than either of S4 or S5, even though the core defect sizes are the same. Surprisingly, the mode spectrum of S6 appears to resemble, in both numbers and positions of modes, the mode spectrum of S2, which is a seven-cell core defect structure. This is contrary to prior art thinking, which indicates that larger core defects should support, proportionately, more modes. The mode marked F6 in P6 is again a degenerate, air-guiding mode that most closely resembles the form of a fundamental mode in a typical standard optical fibre and supports the maximum amount of light in air.

On the basis of the above six examples of different PBG fibre structures, it is clear that the numbers and locations of modes in a mode spectrum are not determined only by size of the core defect, index difference between a core and cladding and wavelength of light; even when the cladding structure is fixed. Taking S1 to S3, for example, it is clear that the locations of modes and, in particular, the number of modes that are likely to be evanescent in air or possibly air-guiding, can be varied significantly by varying the node size, and presence or absence of beads, about the core defect boundary, without the need to vary the core defect size. Additionally, while certain PBG fibre structures that support a greater number of modes – especially potentially air-guiding modes – may be made by increasing the core defect size for any given cladding structure, it also appears possible to increase the core defect size without significantly increasing the number of modes that are supported by the structure. This is surprising and contrary to the thinking in the prior art.

Figure 7 comprises six plots, D1 to D6, which show the mode intensity distributions, over a transverse cross-section of a respective PBG fibre structure, for modes F1 to F6 respectively. The shading of the plots is inverted, such that darker areas represent more intense light than lighter regions. Each plot shows the position and orientation of x and y planes, which correspond to the x and y planes of the structures, as illustrated in Figures 3 and 4. These plots were produced using the results obtained by solving Maxwell's equations for each structure, as described above.

The graphs in Figures 8 and 9 show the mode intensity for modes F1 to F6 along longitudinal planes x and y of D1 to D6 respectively. The intensity values are normalised so that the maximum intensity of the mode is at 0dB on the graph; the y-axis scale being logarithmic. The shaded vertical lines and bands across the graphs coincide with and

represent the glass regions of the actual respective structure along the x and y planes. For the x and y planes, therefore, it is possible to see how the light intensity of the mode varies in the air and glass, and across the glass/air boundaries, of each structure.

Table 1 below shows, for modes F1 to F6, the approximate normalised frequency at which the mode lies within the bandgap of its respective structure and the percentage of light that is in air rather than in the high index silica regions.

Mode Number	Normalised frequency ($\omega\Lambda/c$)	% light in air
F1	13.14	92.8
F2	13.12	97
F3	13.11	97.5
F4	13.05	97.7
F5	13.04	99.6
F6	13.04	99.5

Table 1

The percentage of light in air for modes is found by calculating the integral of the light intensity across only the air regions of the plots in Figure 7 and normalising to the total power. Of course, the plots in Figure 7 represent the intensity across only an inner region of the various PBG fibre structures. Accordingly, the respective percentages of light in air are calculated for the inner regions only and may be slightly different if calculated across entire PBG fibre structures instead. However, as will be seen, the intensities have typically reduced so considerably towards the edges of the plots that any light in regions outside of the inner regions, whether in air, glass or both, is unlikely to have any significant impact on the percentage of light in air values.

Plot D1 shows the mode intensity distribution for the F1 mode, which was found at a normalised frequency $\omega\Lambda/c$ of about 13.14. Plot D1 together with graphs x1 and y1 show that the F1 mode has a generally circular central region in the core defect. The central region of the mode is intense at its centre and decays sharply towards the core defect boundary. There are two intense satellites to the left and right of the central region, coincident with the core defect boundary, and a number of less intense satellites that form a broken ring around the central region. As shown in graph x1, the satellites to the left and right of the central region have slightly higher intensities than the maximum intensity of the central region. It is

significant to note that these intense satellites, along with the larger ones of the less intense satellites around the boundary, appear to coincide with the beads of S1. In addition, it would appear that the remainder of the less intense satellites appear to coincide with the boundary nodes of S1. There is evidence in D1 of some light being concentrated further out from the centre of the structure than the core defect boundary although, as is supported by graphs x1 and y1, the light intensity drops-off rapidly away from the central region. The light that is outside the core defect appears to coincide with cladding nodes.

It is apparent that, for the seven-cell core defect structure S1, a significant amount of light concentrates in the pronounced beads. It is apparent, however, that the F1 mode is air-guiding, with a significant fraction of the light existing in the core defect and with a local intensity minimum of the mode falling within the core defect boundary. The intensity of the light in the glass of the cladding structure decreases significantly moving further away from the core defect boundary.

Plot D2 shows the mode intensity distribution of the F2 mode in the transverse plane of S2. The mode was found at a normalised frequency $\omega\Lambda/c$ of about 13.12. Plot D2 together with graphs x2 and y2 show that the F2 mode has a generally circular central region in the core defect. The central region is intense at its centre and decays sharply towards the core defect boundary. There are six relatively lower intensity satellites about the central region, coincident with the core defect boundary, and lower intensity satellites in glass further out from the central region. The six satellites around the core defect boundary have a lower intensity than the maximum intensity of the central region, in contrast to the intense satellites of plot D1. It is believed that in plot D2 the intensities of the satellites around the core defect boundary are less than in plot D1 due to the removal of the pronounced beads; in-keeping with the observation that, for a seven-cell core defect structure, a significant amount of light concentrates in the pronounced beads.

As with the F1 mode, it is apparent that the F2 mode is air-guiding. It is also apparent that some of the light concentrates in the glass of the cladding structure.

The percentage of light in air for the F2 mode is 97%. This value is significantly larger than the value of 92.8% for the F1 mode even though the core defect size is the same. This increase in the amount of light in air is attributed to the reduction in diameter of the boundary nodes and omission of the beads. Accordingly, it is expected that S2 will have improved loss, non-linearity and mode coupling characteristics compared with S1.

Plot D3 shows the mode intensity distribution of the F3 mode in the transverse plane of S3. The mode was found at a normalised frequency $\omega\Lambda/c$ of about 13.11. The qualitative and quantitative characteristics of the F3 mode, as shown in plot D3 and graphs x3 and y3, very closely match those of the F2 mode. Similarly, the value of the percentage of light in air for the F3 mode is 97.5%, which is very close to the figure for the F2 mode. Accordingly, it is expected that S3 will also have improved loss, non-linearity and mode coupling characteristics compared with S1.

Plot D4 shows the mode intensity distribution of the F4 mode in the transverse plane of S4. The mode was found at a normalised frequency $\omega\Lambda/c$ of about 13.05. Plot D4 together with graphs x4 and y4 show that the F4 mode has a generally circular central region in the core defect. The central region is intense at its centre and decays rapidly towards the core defect boundary, although not as rapidly as in Plots D1 to D3. The central region has a local minimum that falls close to and within the core defect boundary, which means that the central region of the mode in plot D4 has a diameter in the order of two pitches longer than for any of the seven-cell core defect structures.

There are a number of low intensity satellites around the central region in plot D4, which appear to coincide with the boundary nodes of S4. From graphs x4 and y4, these satellites appear to be more than 20dB lower than the peak intensity of the central region. However, it should be noted that the x4 plane does not cross the core defect boundary at a bead, whereas planes x1 to x3 do, which means it is not possible to make a direct comparison of satellite intensity between graph x4 and graphs x1 to x3. The fact that the satellites in plot D4 appear so faint, though, does indicate that they have a significantly reduced intensity compared with satellites in plots D1 to D3.

The F4 mode is apparently air-guiding, with a significant fraction of the light existing in the core defect. Light which is guided outside of the core defect is concentrated in the glass. The percentage of light in air for S4 is 97.7%. This value is an improvement over the highest seven-cell core defect structure value by a small margin (0.2%) and a significant improvement (4.9%) over S1, which has a similar boundary node configuration. Accordingly, it is expected that S4 will have improved loss, non-linearity and mode coupling characteristics compared with S1.

Plot D5 shows the mode intensity distribution of the F5 mode in the transverse plane of S5. The mode was found at a normalised frequency $\omega\Lambda/c$ of about 13.04. Plot D5 together with graphs x5 and y5 show that the F5 mode is very similar in form to the F4 mode, with an

intense central region and only very faint satellites outside of the central region. These satellites appear fainter than those in plot D4. Like the F4 mode, it is apparent that the F5 mode is air-guiding with a significant fraction of the light existing in the core defect.

The percentage of light in air for the F5 mode is 99.6%, which is significantly higher than the value of 97.7% for the F4 mode, even though the core defect sizes are the same. This increase in light in air value is attributed to the reduction in size of the boundary nodes and omission of the beads in S5 when compared with S4. It is expected that S5 will have significantly improved loss, non-linearity and mode coupling characteristics compared with S1 and S4.

Plot D6 shows the mode intensity distribution of the F6 mode in the transverse plane of S6. The mode was found at a normalised frequency $\omega\Lambda/c$ of about 13.04. Plot D6 together with graphs x6 and y6, relating to the F6 mode, very closely match the qualitative and quantitative characteristics of the F5 mode. In addition, the percentage of light in air for the F6 mode is 99.5%, which is similar to the value for the F5 mode. Accordingly, like S5, it is expected that S6 will have significantly improved loss, non-linearity and mode coupling characteristics compared with S1 and S4, while at the same time not supporting a significantly increased number of modes compared with the seven-cell core defect structures of Structures S1 to S3.

Table 2 below provides data for six further exemplary waveguide structures, S7 to S12. The waveguide structures for S7-S12 very closely resemble S3, in that the boundaries have no apparent beads and the boundary nodes have a similar diameter to those in S1. Due to the similarity, and for reasons of brevity herein, S7-S12 are not independently represented in the Figures. The difference between the structures is only in boundary vein thickness, as shown in Table 2. The variations in boundary vein thickness are compensated for by slight variations in core defect diameter.

In Table 2, boundary vein width is normalised relative to the pitch Λ of the structures, which was the same for each structure. Structure S10 has a boundary vein thickness the same as the cladding vein thickness and, hence, was closest in form to S3. For each structure, the position of the mode having the highest percentage of light in air is presented as a frequency that is normalised with respect to the pitch of the structure.

Structure	Boundary Vein Width/Λ	Normalised frequency (ωΛ/c)	% light in air
S7	0.0383	13.11	98.6
S8	0.0438	13.11 (13.29)	98.2 (97.7)
S9	0.0493	13.10	96
S10	0.0548	13.12 (13.28)	96.9 (98.3)
S11	0.0602	13.11	97.3
S12	0.0657	13.11	97.8

Table 2

Discounting for the moment the values in parentheses in Table 2, the modes having the highest percentage of light in air for each structure were found to be ones which most closely resemble the fundamental mode in a standard optical fibre communications system. As can be seen, varying the width of the boundary veins has little effect on the position of the respective modes. In contrast, however, variation in boundary vein thickness has a significant impact on the percentage of light in air for the modes. Within the coarse range of boundary vein thicknesses examined, it can be seen that a candidate as a preferred structure in terms of maximum light in air is S7, which has a boundary vein thickness of around 0.0383Λ (around 70% of the cladding vein thickness). However, a significant improvement over S10 is also seen at a boundary vein thickness of around 0.0438Λ (around 80% of cladding vein thickness). It is worthy of note, also, that the improvement is not linear, with the boundary vein thickness of S9 (around 90% of cladding vein thickness) producing a lower percentage of light in air than either of S10 or S8. In addition, slight improvements over S10 are seen with S11 and S12, which have thicker boundary veins than S10.

Although not described herein in detail, the inventors have found that the mode spectra for structures S7 to S12 vary considerably with varying boundary vein thickness. The variations were at least as marked as those found by varying the boundary node size and bead presence in structures S1 to S3, which are very similar seven-cell core defect structures.

Turning now to the values in parentheses in Table 2, for structure S10, a mode having the values shown was found to be non-degenerate and to exist within the bandgap of S10 to the right of the light line. This mode was found to support the highest fraction of light in air for the structure.

All other modes, which have been shown herein to support the maximum fraction of light in air, have been degenerate.

The intensity distribution for the non-degenerate S10 mode is shown in Figure 10. As can be seen, the mode is characterised by two relatively more intense regions either side of the core defect centre and two relatively less intense regions, bridging the more intense regions, above and below the core defect centre, all within the core defect. There is clearly also some light in the cladding region.

As will be appreciated, a non-degenerate mode may find beneficial application, for example, in a system that is required to have minimal polarisation mode dispersion. This is because, once light has been launched or coupled into the non-degenerate mode, there is no scope for power to couple between degenerate mode pairs, which is the cause of such dispersion in practical systems.

The mode represented by the values in parentheses for S8 was also found to be non-degenerate. However, for this structure, the value of percentage of light in air for this mode was less than the value for the mode that most closely resembles the form of a fundamental mode.

It is expected that there are likely to be a number of non-degenerate modes supported by the present waveguide structures. However, whether or not the modes exist within the bandgap of a particular structure would depend on the relationship between the bandgap and the respective mode spectrum, which, as has been shown, can be extremely sensitive to core size and boundary form at least. The non-degenerate modes typically exist at higher frequencies than the fundamental-like modes. Similarly, the present inventors have found that nineteen cell core defect structures also support these non-degenerate modes.

With reference to Figure 11, prior art structures of the kind exemplified by S1 may be made from a perform 1100 comprising a stack of hexagonal capillaries 1105. The hexagonal capillaries 1105 each have a circular bore. The cladding nodes 160 and boundary nodes 150 (from Figure 1) of the PBG fibre structure result from the significant volume of glass that is present in the perform 1100 wherever the corners 1110, 1115 of neighbouring capillaries meet. The beads 165 are formed from the glass of the inwardly-facing corners 1120 of the capillaries that bound an inner region 1125 of the pre-form 1100, which is to become the core defect region 110 of a PBG fibre structure. These corners 1120, and the two sides of each capillary that meet at the corners, recede due to surface tension as the stack of capillaries is heated and drawn. Such recession turns the two sides and the corner 1120 into a boundary vein 140, with a bead 165. The inner region 1125 may be formed by omitting the inner seven capillaries from the pre-form and, for example, supporting the outer capillaries using

truncated capillaries at either end of the stack, as described in PCT/GB00/01249 (described above) or by etching away glass from inner capillaries in accordance with either PCT/GB00/01249 or US 6,444,133 mentioned above.

While it is possible to adapt the prior art processes in order to make the nineteen-cell core defect S4, which has beads on some of the boundary veins, the present inventors have appreciated that it would be more difficult to manufacture either of S5 or S6 using the prior art techniques. In particular, it would be difficult to control the diameters of boundary nodes using hexagonal cross section capillaries of the kind described with reference to Figure 11. On the other hand, it is difficult to make structures having cladding nodes with diameters which are significantly larger than their respective veins by using purely circular capillaries, especially when the required AFF is high, for example higher than 75%.

The diagram in Figure 12 illustrates one way of forming a preform stack 1200 including a seven cell core region 1210. The core region 1210 is formed by assembling circular cross section capillaries 1220 in a close-packed triangular arrangement around a large diameter core capillary 1230, which is large enough to support capillaries around a region left by removal of seven capillaries: an inner capillary and the six capillaries around the inner capillary. The cladding capillaries 1220 have an outer diameter of about 1mm and a wall thickness of about 0.05mm and the large diameter core capillary 1230 has an outer diameter of about 2.6mm and a wall thickness of about 0.05mm. The large diameter core capillary 1230 supports the cladding capillaries while the stack is being formed and eventually becomes part of the material that forms a core defect boundary.

Interstitial voids 1220 that form at the at the mid-point of each close-packed, triangular group of three cladding capillaries are each packed with a glass rod 1240, which has an outer diameter of about 0.15mm. The rods 1240 that are packed in voids assist in forming cladding nodes, which have a diameter d that is typically significantly greater than the thickness t of the veins that meet at the nodes. Omission of a rod from a void in the cladding leads to the formation of a cladding node that has a relatively smaller diameter, for example closer to the thickness of the respective adjoining veins.

The rods 1240 may be inserted into the voids after the capillaries have been stacked. Alternatively, the stack may be assembled layer by layer, with the rods that rest on top of capillaries being supported by an appropriate jig, for example positioned at either end of the stack, until the next upper layer of capillaries is in place to support those rods. In commercial scale operations, it is apparent that the manual task of forming a preform stack could readily

be automated, using appropriately programmed robots, for example of the kind used in component laying for printed circuit boards.

The interstitial voids 1250 that are formed between the cladding capillaries 1220 and the large diameter capillary 1230 are not packed with any rods, thereby avoiding the formation of beads (of the kind seen in the prior art) and minimising the volume of glass that is available, during drawing of the stack 1200, for formation of boundary nodes. Therefore, by design, the arrangement of capillaries and rods shown in Figure 12 leads to the formation of boundary veins that are generally straight and smooth along their lengths between nodes (although the thickness varies slightly, with a thinnest region at their mid-points between nodes).

The SEM images in Figure 13 show the inner region of fibres made using a seven cell preform stack of the kind illustrated in Figure 12. Both fibres resemble structure S3. As can be seen, the fibres have core boundary regions of glass comprising twelve veins. The veins are generally smooth along their lengths – with their thinnest points typically at their mid-points - and they clearly do not have beads along any veins, in contrast to the prior art structure illustrated in Figure 1. The lack of beads along the boundary veins is a function of making a fibre from a stack according to Figure 12. It would, in contrast, be difficult to form a PBG fibre having similar smooth boundary veins by using a stack comprising hexagonal cladding capillaries. Both fibres have boundary veins that conform to the relationship: $t < d_L$ and $t < d_F$ is true for more than half of the boundary veins; and $l \geq x(d_L+d_F)$ is true for at least one boundary vein, where $x \geq 0.6$ and d_L, d_F are the diameters of the leading and following nodes respectively for each boundary vein.

As can be seen, the fibre in Figure 13a has slightly thicker boundary and cladding veins than the fibre in Figure 13b. R for the fibre in Figure 13b is clearly larger than R for the fibre in Figure 13a. In other words, the cladding cells in Figure 13b are rounder than the cladding cells in Figure 13a. The core defect of the fibre in Figure 13b has a larger diameter than the core defect of the fibre in Figure 13a, even though both fibres have a seven-cell core defect. This is due to the core defect of the fibre in Figure 13b having been more highly pressurised during the drawing process than the core defect of the fibre in Figure 13a. One consequence of this is that the hexagonal boundary cells in Figure 13b are slightly squashed in the radial direction and expanded in the azimuthal direction, which causes a significant perturbation in the cladding structure to propagate radially outward from the centre of the core defect, compared with the structure in Figure 13a.

Another exemplary preform stack 1400, according to an embodiment of the present invention, is illustrated in Figure 14. In this case a core region 1410 is defined by a larger diameter capillary 1430, having an outer diameter of around 4.5mm, which supports cladding capillaries 1420 around a region left by removal of nineteen capillaries: an inner capillary, the six capillaries around the inner capillary and the twelve capillaries around the six capillaries. The dimensions of the cladding capillaries 1420 and rods 1440 are the same as in the stack illustrated in Figure 12.

An SEM image of an inner region of a PBG fibre, drawn from a preform of the kind illustrated in Figure 14, is shown in Figure 15. The structure shown in the image resembles the fibre S6, which has no apparent beads and the boundary nodes 150 are smaller in diameter than the cladding nodes 160. Again, the core boundary veins of the PBG fibre are generally straight and smooth by design, and conform to the relationship: $t < d_L$ and $t < d_F$ is true for more than half of the boundary veins; and $l \geq x(d_L+d_F)$ is true for at least one boundary vein, where $x \geq 0.6$ and d_L, d_F are the diameters of the leading and following nodes respectively for each boundary vein.

The fibre represented in Figure 15 has the transmission loss characteristic shown in the graph in Figure 16. The measurements were made using an optical spectrum analyser and a white light source (both from ANDO™). The measured fibre length was 300 metres, cut back to twenty metres. As shown on the graph, the fibre exhibits a transmission bandwidth of nearly 100nm and a minimum loss of around 11dB/km at an operating wavelength of between 1580nm and 1590nm. These results are an improvement over the known prior art lowest loss of 13dB/km. In addition, it is clear from the SEM image in Figure 15 that the structural homogeneity of the fibre still has room for improvement; the holes around the core defect boundary being significantly deformed compared with a perfect cladding hole arrangement, for example of the kind illustrated by fibre structure S6. It is anticipated that improved fibre structures and attendant loss figures will be achieved through further experimentation.

The cladding regions of the fibres in Figures 13 and 15 have AFF values of between 0.85 and 0.92. Lower and higher values of AFF are achievable using a similar preform construction and varying cladding capillary wall thickness. The AFF value can also be varied for a given preform stack by drawing the fibre while pressurising the cladding and core holes at an appropriate level. A relatively higher pressure will tend to cause the resulting fibre to have a higher AFF, relative to that of the preform, while a relatively lower pressure will tend to cause the resulting fibre to have a lower AFF. In any case, it is necessary to pressurise the

core hole to a lower level than the cladding holes, since a lower pressure is required to counteract the surface tension in a relatively large hole than in a relatively small hole during drawing.

Prior to being drawn into fibre, the stacks shown in Figures 12 and 14 are over-clad with a further, relatively thick walled capillary (for example, as illustrated in Figure 20), which is large enough to contain the stack and, at the same time, small enough to hold the capillaries and rods in place. The entire over-clad stack is then heated and drawn into a fused pre-form, during which time all the interstitial voids at least partially collapse due to surface tension. The pre-form is, again, over-clad with a final, thick silica cladding (not shown) and is heated and drawn into optical fibre in a known way, in the process of which any remaining interstitial voids should collapse entirely. If surface tension alone is insufficient to collapse the interstitial voids, a vacuum may be applied to the interstitial voids of the pre-form during drawing, for example according to the process described in WO 00/49436 (The University of Bath).

The thickness of the core boundary in a fibre resulting from a preform of the kind illustrated in Figure 12 is controlled in part by selecting an appropriate thickness of the initial core capillary. A limiting factor in reducing the wall thickness would typically be the ability to make such a respective thin-walled capillary.

An alternative way to reduce the size of boundary nodes 150, and decrease the boundary wall thickness, is by omitting a large diameter capillary altogether. As illustrated in Figure 17, the stack of cladding capillaries 1705 and rods 1725 is supported around an insert 1715, for example made from graphite, platinum, tungsten or a ceramic material, which is in a central region 1710 of the stack and which has a higher melting point than silica glass and, preferably, a higher coefficient of thermal expansion. The stack 1700, including the insert 1715, is heated to allow the capillaries 1705 and rods 1725 to fuse into a pre-form. The pre-form is then allowed to cool and the insert 1715 is removed. It will be apparent that, at this point, the core defect would take on the hexagonal shape of the insert. An advantage of using an insert material having a higher coefficient of thermal expansion than silica is that, when the pre-form and insert 1715 are heated, the insert expands and increases the area of the central region 1710. When permitted to cool down again, the insert 1715 shrinks back down to its original size and the silica solidifies leaving an inner region that is larger than the insert. The insert, which as a result is loose-fitting in the central region, may then be removed readily from the pre-form with reduced risk of damaging or contaminating the pre-form. The

resulting pre-form is then heated and drawn in the usual way to form a PBG fibre. During the drawing step, it will be appreciated that the corners of the hexagonal core defect will, by virtue of surface tension, retract and flatten off, leaving a twelve-sided core defect closely resembling that in structure S5. A similar procedure, using a smaller insert to form a seven-cell core defect pre-form, could be used to make a structure closely resembling structure S2.

On the basis of the foregoing discussion, it will be apparent to the skilled person that the use of an insert in the formation of a pre-form is not limited to formation of nineteen-cell core defect structures and could be applied to making pre-forms for other core defect sizes, for example one-cell, seven-cell or thirty-seven cell core defect structures. Indeed, all of these structures have a core defect notionally centred on a primitive unit cell. Of course, a structure could be made, which has a core defect centred on a notional node and which lies at the mid-point of a triangular arrangement of three notional neighbouring primitive unit cells. For example, the core defect could be made by removing three primitive unit cells that are arranged in a regular triangle, or three primitive unit cells as well as the nine primitive unit cells around the three primitive unit cells, etc. Further, inserts having, for example, star-shaped, elongate, circular, square, rectangular, elliptical or irregular cross sections, or any other practical shape for that matter (for example, see the exemplary insert in Figure 19, which is a star-shaped insert), could be applied to making pre-forms for fibre structures. Additionally or alternatively, inserts could be made by combining plural pieces. For example, an insert could be 'stacked' into a pre-form 1800 using elongate members 1815 having similar cross sections to the capillaries, as shown in Figure 18. As such, the insert could be made to match the cladding very closely, which may prove advantageous.

A further alternative way to reduce the size of boundary nodes 150 and avoid beads 165 is by using the process described in PCT/GB00/01249 (described above), wherein the inner capillaries are replaced by truncated capillaries, which support the outer capillaries at either end of the stack. The stack may be drawn to an optical fibre in the normal way, and the parts of the fibre incorporating the truncated capillary material may be discarded. In principle, truncated capillaries may also be used to support the stack part way along its length.

The diagram in Figure 20 illustrates a small portion of an outer region of a preform stack 2000 made from circular cross section capillaries 2020. In this embodiment, the entire stack is contained in a large circular cross section capillary tube 2070, having a generally circular bore, which is large enough to receive the entire assembled stack as a sliding fit. As shown, interstitial voids 2075 form between the edges of the stack and the internal surface of

the large capillary. It has been found beneficial to pack these interstitial voids with circular cross section packing rods 2080, having various sizes selected to support all cladding capillaries in their appropriate positions within the large capillary. These rods melt and fuse with the large circular capillary to form a homogenous outer layer of glass that surrounds the microstructured inner region.

The skilled person will appreciate that the various structures described above may be manufactured using a manufacturing process described with reference to Figures 11-20. Alternatively, rather than using a stacking and drawing approach to manufacture, a pre-form may be made using a known extrusion process and then that pre-form may be drawn into an optical fibre in the normal way.

In addition, the skilled person will appreciate that while the examples provided above relate exclusively to PBG fibre cladding structures comprising triangular arrays, the present invention is in no way limited to such cladding structures. For example, the invention could relate equally to square, hexagonal, Kagome or other structures, including structures that are not close-packed. In general, the inventors propose that given a cladding structure that provides a PBG and a core defect in the cladding structure that supports guided modes, the form of the boundary at the interface between the core defect and the cladding structure will have a significant impact on the characteristics of the waveguide, as described herein.

The skilled person will also appreciate that, regarding the exemplary PBG waveguide structures described hereinabove, some structures are embodiments of the present invention whereas other structures are not. The structures that are not embodiments of the present invention are included for comparison purposes in order to assist in demonstrating the differences in characteristics between different structures. Additionally, the skilled person will appreciate that the structures described herein fit on a continuum comprising a huge number of different structures, for example having different combinations of core defect size, boundary node size, boundary vein thickness and, in general, boundary and cladding form. Clearly, it would be impractical to illustrate each and every variant of PBG waveguide structure herein. As such, the skilled person will accept that the present invention is limited in scope only by the present claims.

CLAIMS

1. A photonic bandgap optical waveguide comprising:

a photonic bandgap structure, having a plane cross section and a length dimension that extends perpendicular to the plane cross section, the photonic bandgap structure, in the plane cross section, comprising a substantially periodic array of relatively low refractive index regions, being separated from one another by relatively high refractive index regions, which extend along the photonic bandgap structure in the length dimension, the array having a characteristic primitive unit cell and a pitch Λ and comprising more than a seventy percent fraction by volume of relatively low refractive index regions; and

a core defect, surrounded by the photonic bandgap structure, the core defect comprising a region of relatively low refractive index having a plane cross section and a length dimension that extends perpendicular to the plane cross section, said plane cross section and length dimension being parallel to the same dimensions of the photonic bandgap structure, the area of the core defect region of relatively low refractive index being greater than sixteen times the area of the primitive unit cell.

2. The waveguide according to claim 1, wherein, in the plane cross section, the core defect region of relatively low refractive index is large enough to contain at least sixteen substantially whole primitive unit cells.

3. The waveguide according to claim 1 or claim 2, wherein, in the plane cross section, the core defect region of relatively low refractive index is substantially equal to nineteen times the area of the primitive unit cell.

4. The waveguide according to claim 1 or claim 2, wherein, in the plane cross section, the core defect region of relatively low refractive index is large enough to contain at least nineteen substantially whole primitive unit cells.

5. The waveguide according to claim 4, wherein, in the plane cross section, the area of the core defect region of relatively low refractive index is greater than thirty times the area of the primitive unit cell.

6. The waveguide according to any one of the preceding claims, wherein, in the plane cross section, the core defect region of relatively low refractive index has at least two-fold rotational symmetry.

7. The waveguide according to any one of the preceding claims, wherein, in the plane cross section, the relatively low refractive index regions of the photonic bandgap structure are arranged in a substantially triangular array in the photonic bandgap structure.

8. The waveguide according to any one of the preceding claims, wherein the primitive unit cell is centred on a single relatively low refractive index region, that being the largest relatively low refractive index region in the primitive unit cell.

9. The waveguide according to any one of the preceding claims, wherein, in the plane cross section, the area of the core defect region of relatively low refractive index is substantially equal to the area of a first primitive unit cell, a first group of all primitive unit cells that surround the first primitive unit cell and a second group of all primitive unit cells that surround said first group of primitive unit cells.

10. The waveguide according to any one of the preceding claims, wherein, in the plane cross section, the core defect has a form that would be obtained by the omission or removal of relatively high refractive index regions from a first primitive unit cell, a first group of all primitive unit cells that surrounded the first primitive unit cell and a second group of all primitive unit cells that surrounded said first group of primitive unit cells.

11. A photonic bandgap optical waveguide comprising:

a photonic bandgap structure, having a plane cross section and a length dimension that extends perpendicular to the plane cross section, the photonic bandgap structure, in the plane cross section, comprising a substantially periodic array of relatively low refractive index regions, being separated from one another by relatively high refractive index regions, which extend along the photonic bandgap structure in the length dimension, the array having a characteristic primitive unit cell and a pitch Λ, the primitive unit cell being centred on a single relatively low refractive index region, that being the largest relatively low refractive index region in the primitive unit cell; and

a core defect, surrounded by the photonic bandgap structure, the core defect comprising a region of relatively low refractive index having a plane cross section and a length dimension that extends perpendicular to the plane cross section, said plane cross section and length dimension being parallel to the same dimensions of the photonic bandgap structure, wherein the core defect has a form that would be obtained by the omission or removal of relatively high refractive index regions from a first primitive unit cell, a first group of all primitive unit cells that surrounded the first primitive unit cell and a second group of all primitive unit cells that surround said first group of primitive unit cells.

12. The waveguide according to claim 11, wherein the photonic bandgap structure comprises a substantially periodic, triangular array of relatively low refractive index regions.

13. The waveguide according to claim 12, wherein the core defect has a form that would be obtained by the omission or removal of relatively high refractive index regions from a first primitive unit cell, the six primitive unit cells that surround the first primitive unit cell and the twelve primitive unit cells that surround said six primitive unit cells.

14. The waveguide according to any one of the preceding claims, wherein, in the plane cross section, the relatively low refractive index regions of the photonic bandgap structure are separated from one another by relatively high refractive index veins that are joined at nodes, each node having a diameter and each vein having a length and a thickness, at the mid-point along the length, and being joined at each end to a node.

15. The waveguide according to claim 14, wherein, in the plane cross section, at least some of the nodes within the photonic bandgap structure have diameters that are significantly larger than the thickness of the veins that meet at the nodes.

16. The waveguide according to claim 15, wherein, in the plane cross section, substantially all of the nodes within the photonic bandgap structure have diameters that are significantly larger than the thickness of the veins that meet at the nodes.

17. The waveguide according to claim 15 or claim 16, wherein, in the plane cross section, said nodes that are significantly larger than the thickness of the veins that meet at the nodes have a diameter that is at least 1.5 times the thickness of the veins.

18. The waveguide according to any one of claims 15 to 17, wherein, in the plane cross section, said nodes that are significantly larger than the thickness of the veins that meet at the nodes have a diameter that is at least twice the thickness of the veins.

19. The waveguide according to any one of the preceding claims, further comprising, in the plane cross section, a boundary at the interface between the core defect and the photonic bandgap structure, the boundary comprising a plurality of relatively high refractive index veins that are joined at nodes, each node having a diameter and each vein having a length and a thickness, at the mid-point along the length, and being joined at each end to a node.

20. The waveguide according to claim 19, wherein, in the plane cross section, a fraction of nodes which have diameters that are significantly larger than the thickness of the veins that meet at the nodes is less on the boundary than in a similar region of the photonic bandgap structure.

21. The waveguide according to claim 19 or claim 20, wherein, in the plane cross section, the boundary includes substantially no nodes which have diameters that are significantly larger than the thickness of the veins that meet at the nodes.

22. The waveguide according to any one of claims 1 to 18, further comprising, in the plane cross section, a boundary at the interface between the core defect and the photonic bandgap structure, the boundary comprising a plurality of relatively high refractive index boundary veins joined end-to-end around the boundary between boundary nodes, each boundary vein having a length l and a thickness t, at the mid-point along the length l, and being joined between a leading boundary node and a following boundary node, and each boundary node having a diameter and being joined between two boundary veins and to a relatively high refractive index region of the photonic bandgap structure, wherein, in the plane cross section, around the boundary:

$t < d_L$ and $t < d_F$ is true for more than half of the boundary veins; and

$l \geq x(d_L+d_F)$ is true for at least one boundary vein,

where $x \geq 0.6$ and d_L, d_F are the diameters of the leading and following nodes respectively for each vein.

23. The waveguide according to claim 22, wherein $l \geq x(d_L+d_F)$ is true for a plurality of the boundary veins.

24. The waveguide according to claim 22 or claim 23, wherein $x \geq 0.8$.

25. The waveguide according to any one of claims 22 to 24, wherein, in the plane cross section, the thinnest point along at least some of the boundary veins is substantially at the mid-point.

26. The waveguide according to any one of claims 22 to 25, wherein, in the plane cross section, the thickness at the midpoint of a plurality of the boundary veins is less than 0.1Λ.

27. The waveguide according to any one of claims 22 to 26, wherein, in the plane cross section, the thickness at the mid-point of a plurality of the boundary veins is less than 0.049Λ.

28. The waveguide according to any one of claims 22 to 27, wherein, in the plane cross section, at least some boundary nodes have diameters that are significantly smaller than at least some nodes in the photonic bandgap structure.

29. The waveguide according to any one of claims 22 or claim 28, wherein, in the plane cross section, substantially all boundary nodes have diameters that are significantly smaller than a significant proportion of all nodes in the photonic bandgap structure.

30. The waveguide according to any one of the preceding claims, wherein at least some of the relatively low refractive index regions are voids filled with air or under vacuum.

31. The waveguide according to any one of the preceding claims, wherein at least some of the relatively high refractive index regions comprise silica glass.

32. The waveguide according to any one of claim 19 to 29, wherein at least some of the boundary veins are substantially straight.

33. The waveguide according to any one of the preceding claims, wherein the proportion by volume of relatively low refractive index regions in the photonic bandgap structure is greater than 75%.

34. The waveguide according to any one of the preceding claims, which supports a mode in which greater than 95% of the mode power in the waveguide is in relatively low refractive index regions.

35. The waveguide according to any one of the preceding claims, which supports a mode having a mode profile that closely resembles the fundamental mode of a standard, single mode optical fibre.

36. The waveguide according to claim 35, wherein said mode supports a maximum amount of the mode power in relatively low refractive index regions compared with other modes that are supported by the waveguide.

37. The waveguide according to any one of the preceding claims, which supports a core-guided, non-degenerate mode.

38. The waveguide according to any one of the preceding claims, which supports plural core-guided modes.

39. The waveguide according to any one of the preceding claims, having an operating wavelength, wherein the pitch of the photonic band-gap structure is greater than the operating wavelength.

40. An optical fibre comprising a waveguide according to any one of the preceding claims.

41. A transmission line for carrying data between a transmitter and a receiver, the transmission line including along at least part of its length a fibre according to claim 40.

42. A preform for making a photonic bandgap optical waveguide, the preform comprising:

a first part for forming a photonic bandgap structure of the photonic bandgap optical waveguide, the first part having a plane cross section and a length dimension that extends perpendicular to the plane cross section and, in the plane cross section, a substantially periodic array of relatively low refractive index regions, being separated from one another by relatively high refractive index regions, which extend along the first part in the length dimension, the array having a characteristic primitive unit cell and a pitch; and

a relatively low-index region which becomes a core defect in the photonic bandgap structure of the photonic bandgap optical waveguide, the relatively low index region being surrounded by said first part and having a plane cross section and a length dimension that extends perpendicular to the plane cross section, said plane cross section and length dimension being parallel to the same dimensions of said first part, the area of the relatively low index region being greater than sixteen times the area of the primitive unit cell.

43. A preform for making a photonic bandgap optical waveguide, the preform comprising:

a first part for forming a photonic bandgap structure of the photonic bandgap optical waveguide, the first part having a plane cross section and a length dimension that extends perpendicular to the plane cross section and, in the plane cross section, a substantially periodic array of relatively low refractive index regions, being separated from one another by relatively high refractive index regions, which extend along the first part in the length dimension, the array having a characteristic primitive unit cell and a pitch, the primitive unit cell being centred on a single relatively low refractive index region and encompassing no more than one relatively low refractive index region; and

a relatively low-index region which becomes a core defect in the photonic bandgap structure of the photonic bandgap optical waveguide, the relatively low index region being surrounded by said first part and having a plane cross section and a length dimension that extends perpendicular to the plane cross section, said plane cross section and length dimension being parallel to the same dimensions of said first part, the core defect has a form that would be obtained by the omission or removal of relatively high refractive index regions from a first primitive unit cell, a first group of all primitive unit cells that surround the first

primitive unit cell and a second group of primitive unit cells that surround said first group of primitive unit cells.

44. The preform according to claim 42 or claim 43, wherein the photonic bandgap structure comprises a substantially periodic, triangular array of relatively low refractive index regions.

45. The preform according to claim 44, wherein the core defect has a form that would be obtained by the omission or removal of relatively high refractive index regions from a first primitive unit cell, the six primitive unit cells that surround the first primitive unit cell and the twelve primitive unit cells that surround said six primitive unit cells.

46. The preform according to any one of claims 42 to 45, wherein the first part comprises a stack of elongate members.

47. The preform according to claim 46, wherein at least some of the elongate members comprise, in the plane cross section, a relatively low refractive index inner region and a relatively high refractive index outer region, which surrounds the inner region.

48. The preform according to claim 47, wherein the at least some elongate members comprise capillaries.

49. The preform according to any one of claims 46 to 48, wherein at least some of the elongate members comprise solid rods.

50. The preform according to any one of claims 42 to 45, wherein the first part comprises a single, substantially rigid structure.

51. The preform according to claim 50, wherein the preform is formed by a process comprising extrusion.

52. A method of forming a photonic bandgap optical waveguide comprising the steps of forming the preform as claimed in any one of claims 42 to 51 and heating and drawing the preform into a photonic bandgap optical waveguide.

53. A method of forming a photonic bandgap optical waveguide comprising the steps:

forming a preform stack by stacking a plurality of elongate elements into a periodic array of elements, the elongate elements comprising a relatively low refractive index elongate inner region enclosed by a relatively high refractive index outer region;

omitting, or substantially removing from an inner region of the stack, a first element, a first number comprising all elements from around said first element and a second number comprising all elements from around said first number of elements; and

heating and drawing the stack, in one or more steps, into a photonic bandgap optical waveguide, characterised by a photonic bandgap structure that surrounds a core defect, the photonic bandgap structure having a plane cross section and a length dimension that extends perpendicular to the plane cross section and comprising, in the plane cross section, a periodic, triangular array of relatively low refractive index regions, being separated from one another by relatively high refractive index regions, which extend along the photonic bandgap structure in the length dimension.

54. The method according to claim 53, wherein the preform stack comprises a substantially periodic, triangular array of elongate elements.

55. The method according to claim 54, wherein the inner region of the stack is formed by omission or substantial removal of a first element, the six elements that surround the first elements and the twelve elements that surround said six elements.

56. The method according to any one of claims 53 to 55, wherein the elements have a generally hexagonal transverse cross section

57. The method according to any one of claims 53 to 55, wherein the elements have a generally circular transverse cross section.

58. The method according to claim 57, wherein, first elongate interstitial voids are formed between elements.

59. The method according to claim 58, including the additional step of introducing further elongate elements into at least some of the first interstitial voids.

60. The method according to claim 59, wherein at least some of the further elongate elements comprise rods.

61. The method according to claim 59 or claim 60, wherein at least some of the further elongate elements comprise capillaries.

62. The method according to any one of claims 59 to 61, wherein further elongate elements are introduced into substantially all of the first interstitial voids.

63. The method according to any one of claims 53 to 62, including the additional step of introducing an inner elongate element into the inner region to support the elements around the inner region.

64. The method according to claim 63, wherein second interstitial voids are formed between the elements around the inner region and the inner elongate element.

65. The method according to claim 64, including the additional step of introducing additional elongate elements into at least some of the second interstitial voids.

66. The method according to claim 65, wherein at least some of the additional elongate elements comprise rods.

67. The method according to claim 65 or claim 66, wherein at least some of the additional elongate elements comprise capillaries.

68. The method according to any one of claims 65 to 67, wherein a reduced fraction of the additional elements are introduced into the second interstitial voids compared with the number of elements that are introduced into a similar configuration of first interstitial voids.

69. A method according to claim 64, wherein no additional elongate elements are introduced into the second interstitial voids.

70. A method according to any one of claims 65 to 68, wherein at least some of the additional elongate elements that are introduced into the second interstitial voids have a smaller cross sectional area than the elongate elements that are introduced into the first interstitial voids.

71. The method according to any one of claims 63 to 70, wherein the inner elongate element has a relatively low refractive index elongate inner region enclosed by a relatively high refractive index outer region, which becomes part of the photonic bandgap optical waveguide.

72. The method according to any one of claims 63 to 70, wherein the further elongate element comprises a material that has higher melting point and coefficient of thermal expansion than the relatively high refractive index material in the elongate elements.

73. The method according to claim 72, further comprising the steps of:

heating the preform stack in order to fuse the elongate elements around the further elongate element;

cooling the preform stack; and

removing the further elongate element from the preform stack prior to heating and drawing the preform stack.

74. The method according to any one of claims 53 to 73, wherein at least some of the relatively low refractive index regions comprise air or are under vacuum.

75. The method according to any one of claims 53 to 73, wherein at least some of the relatively low refractive index regions are voids filled with a gas other than air or a liquid.

76. The method according to any one of claims 53 to 75, wherein at least some of the relatively high refractive index regions comprise silica glass.

77. An optical fibre comprising a photonic bandgap optical waveguide made by the method of any one of claims 53 to 76.

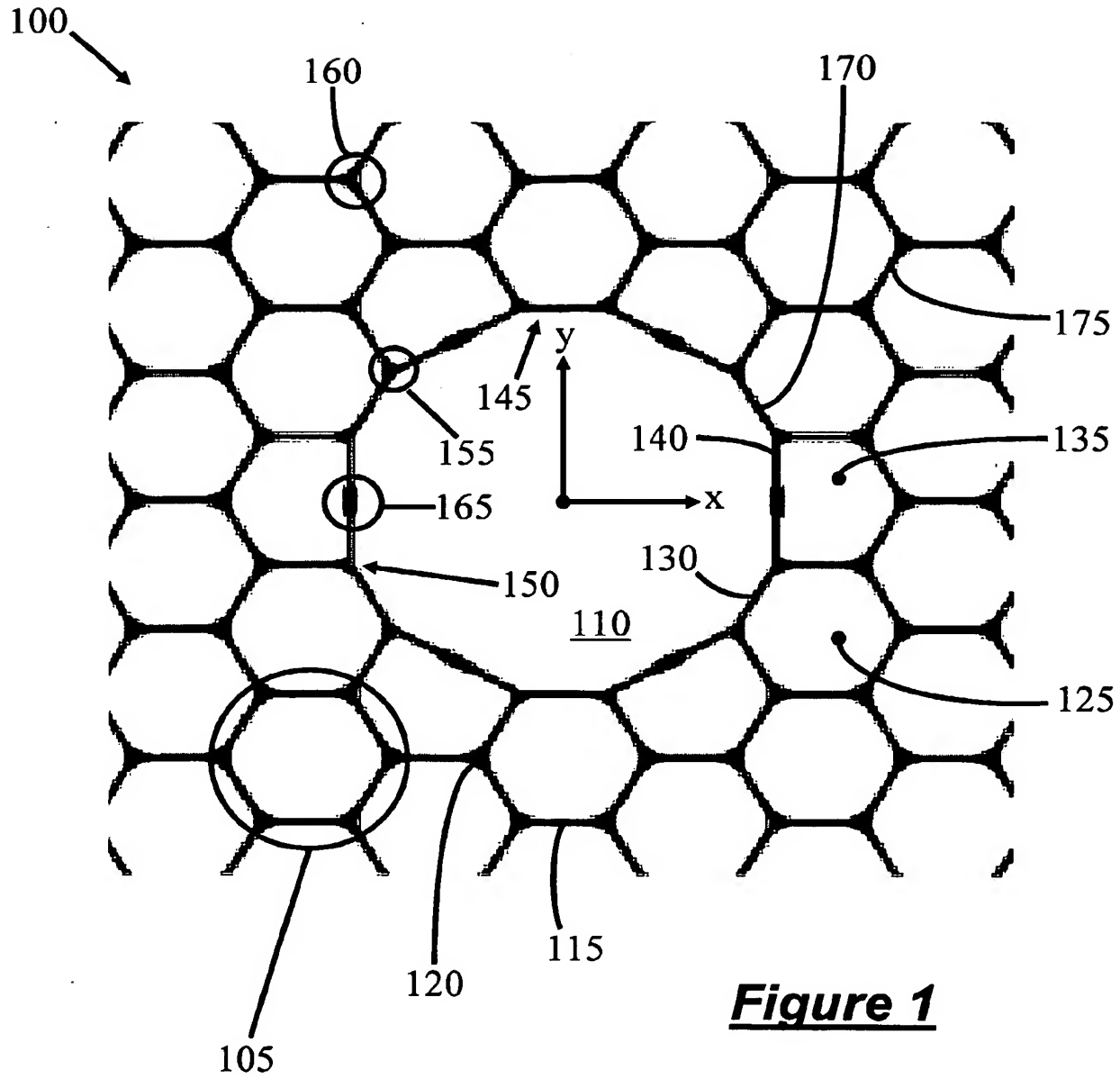
100
160
170
175
y
145
155
140
135
165
x
150
130
110
125
115
120
105

Figure 1

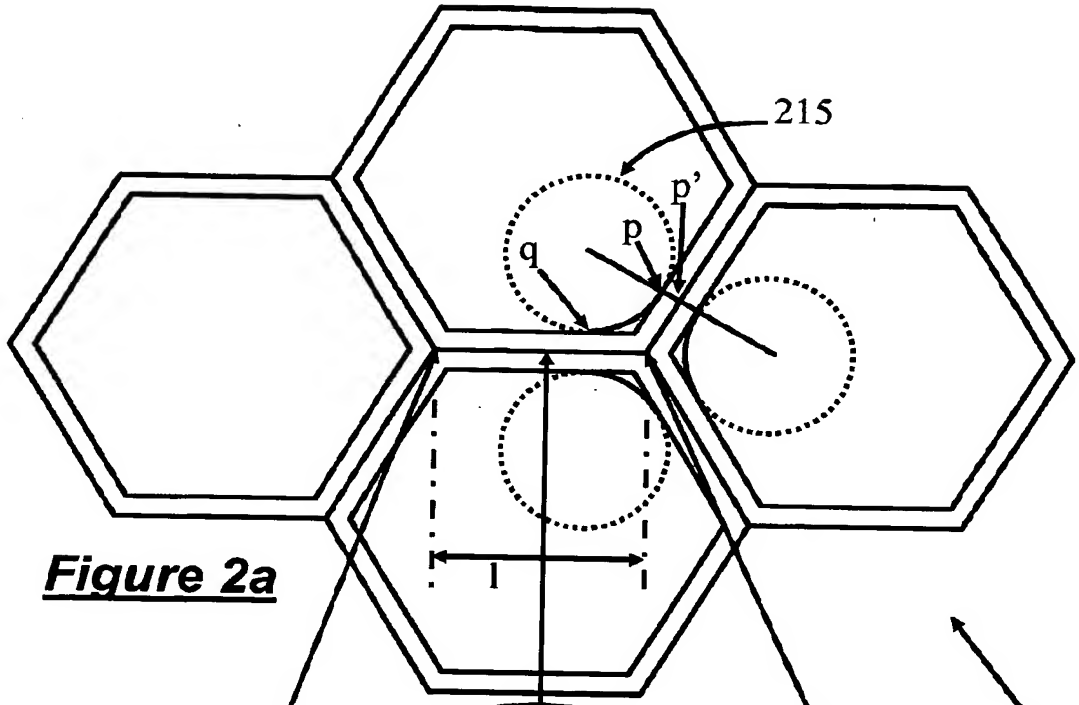

Figure 2a

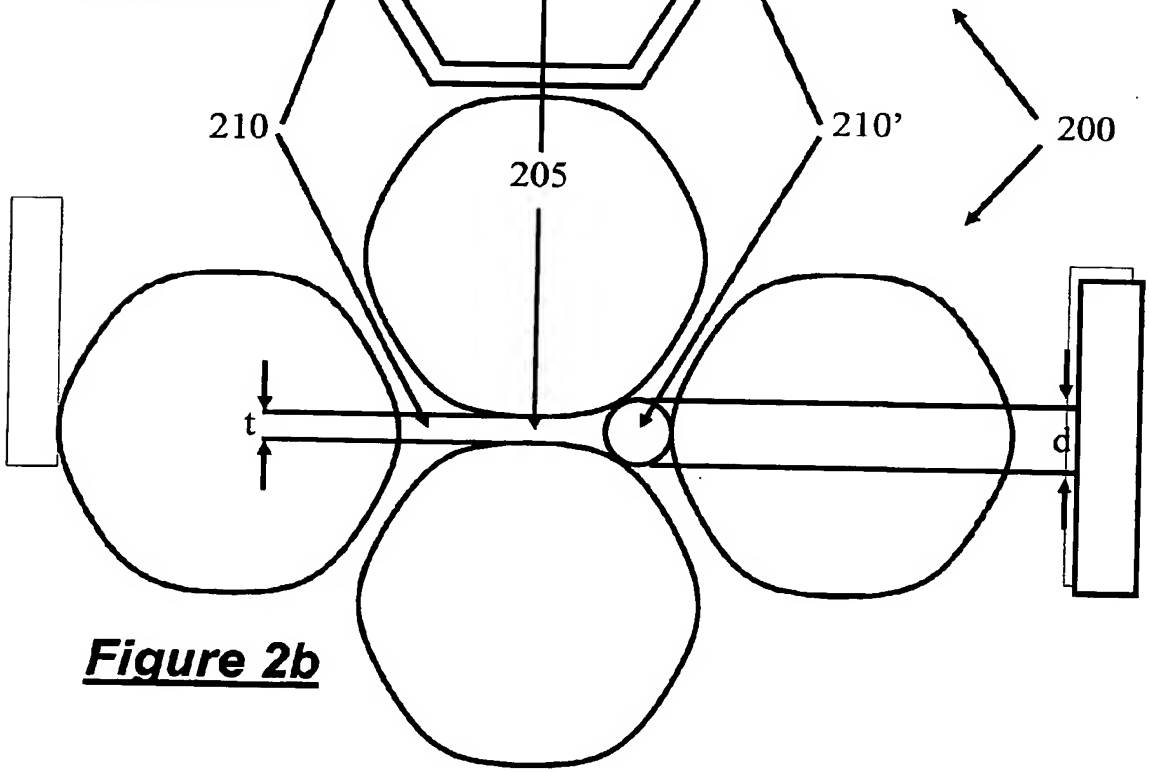

Figure 2b

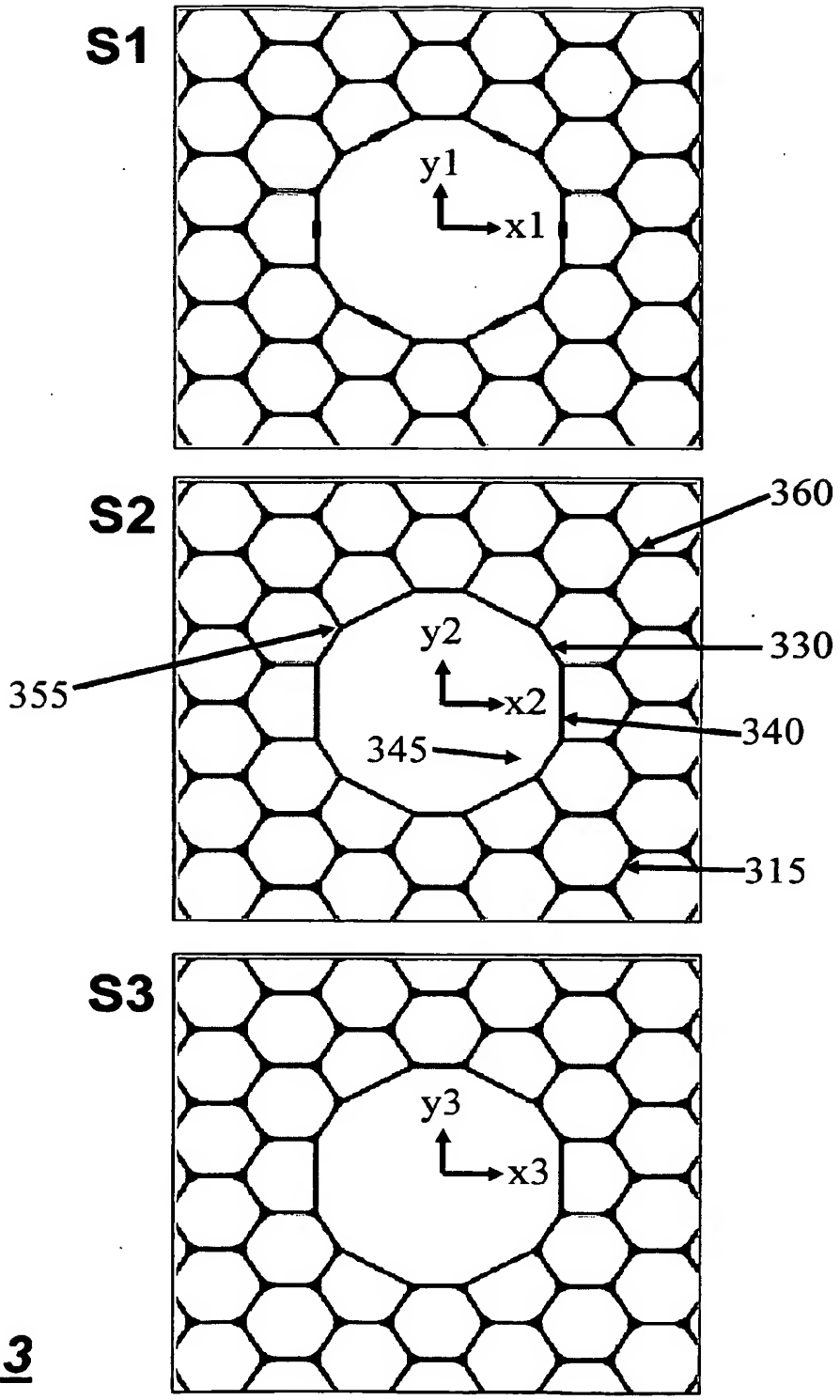

Figure 3

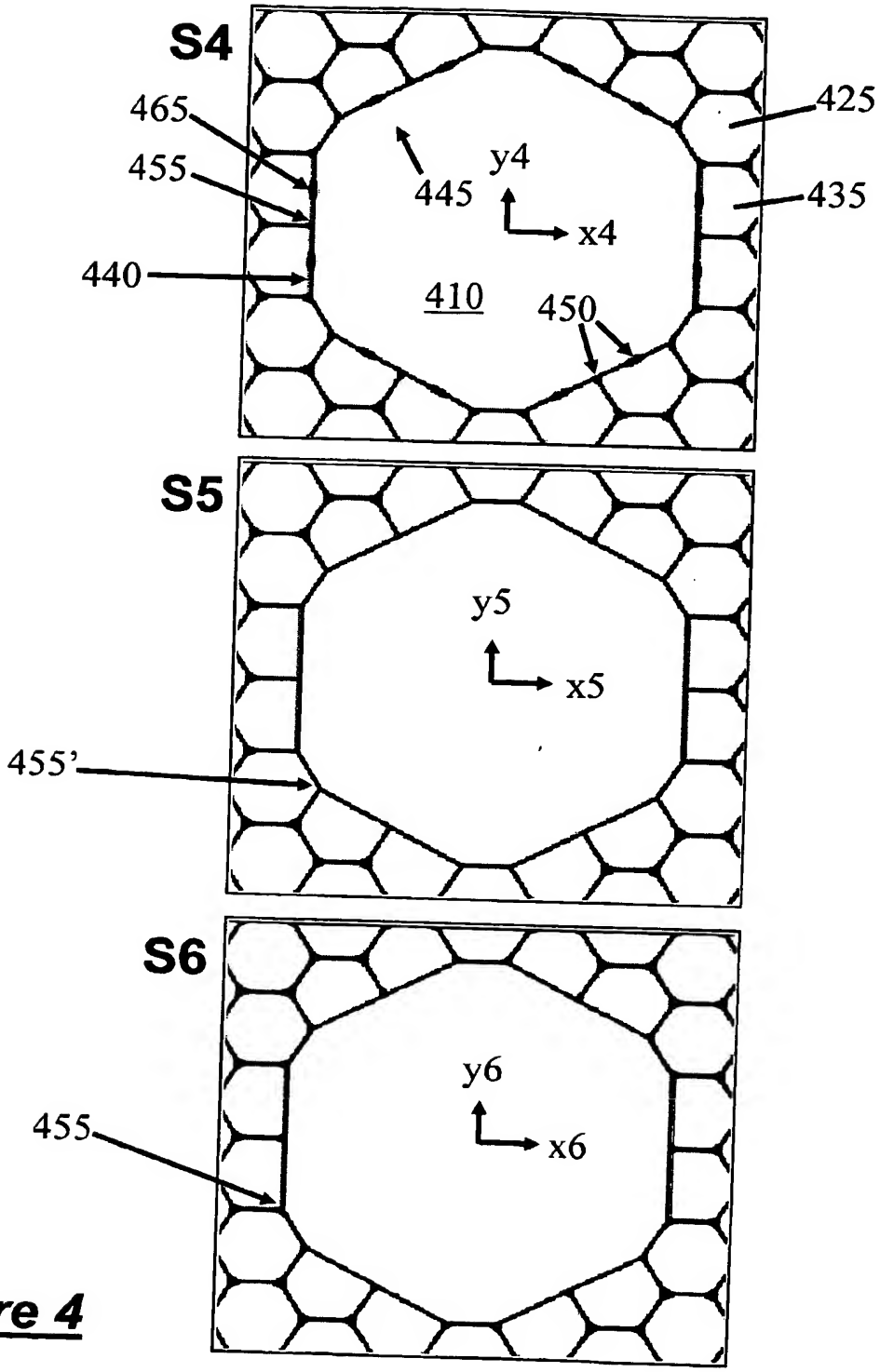

Figure 4

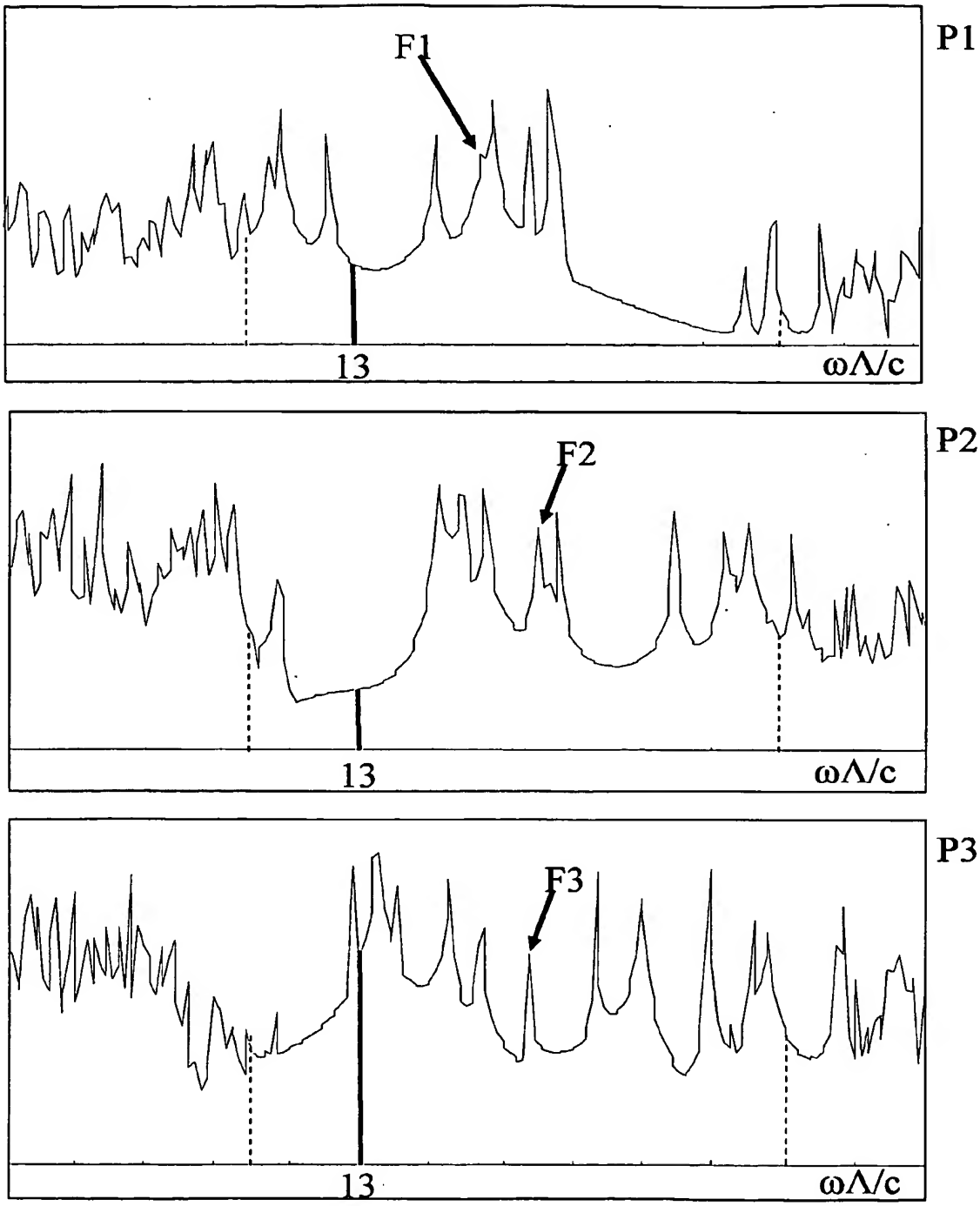

Figure 5

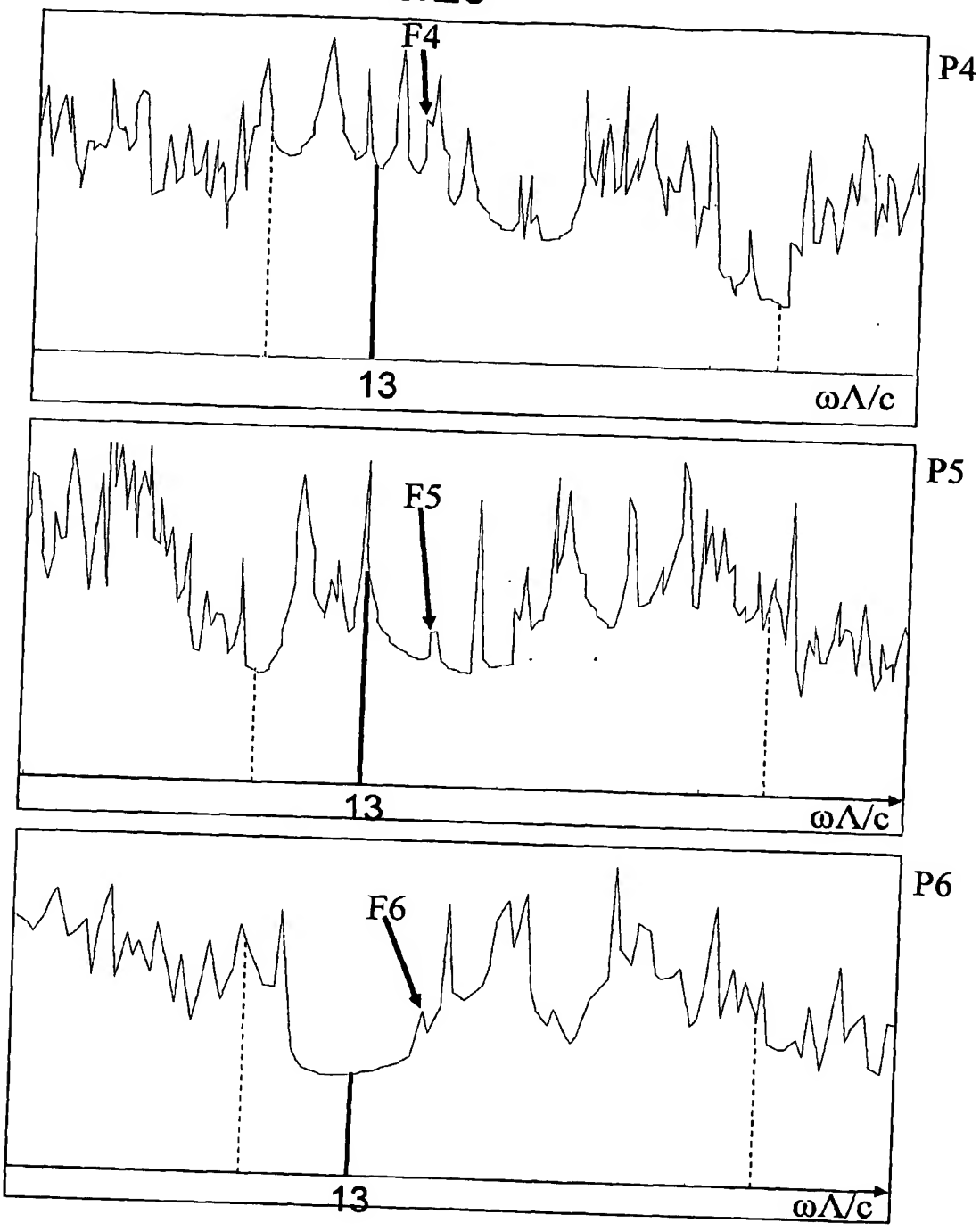

Figure 6

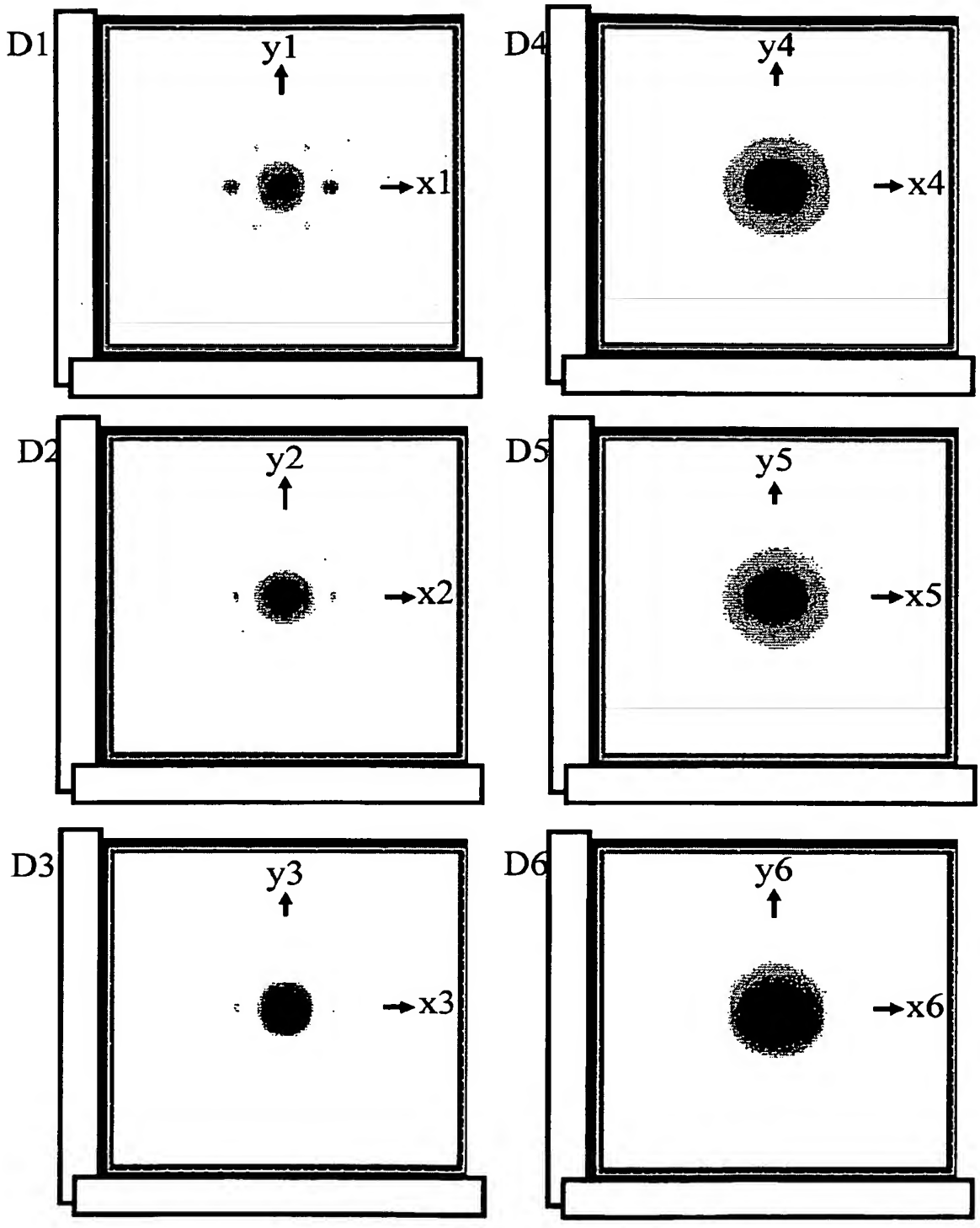

Figure 7

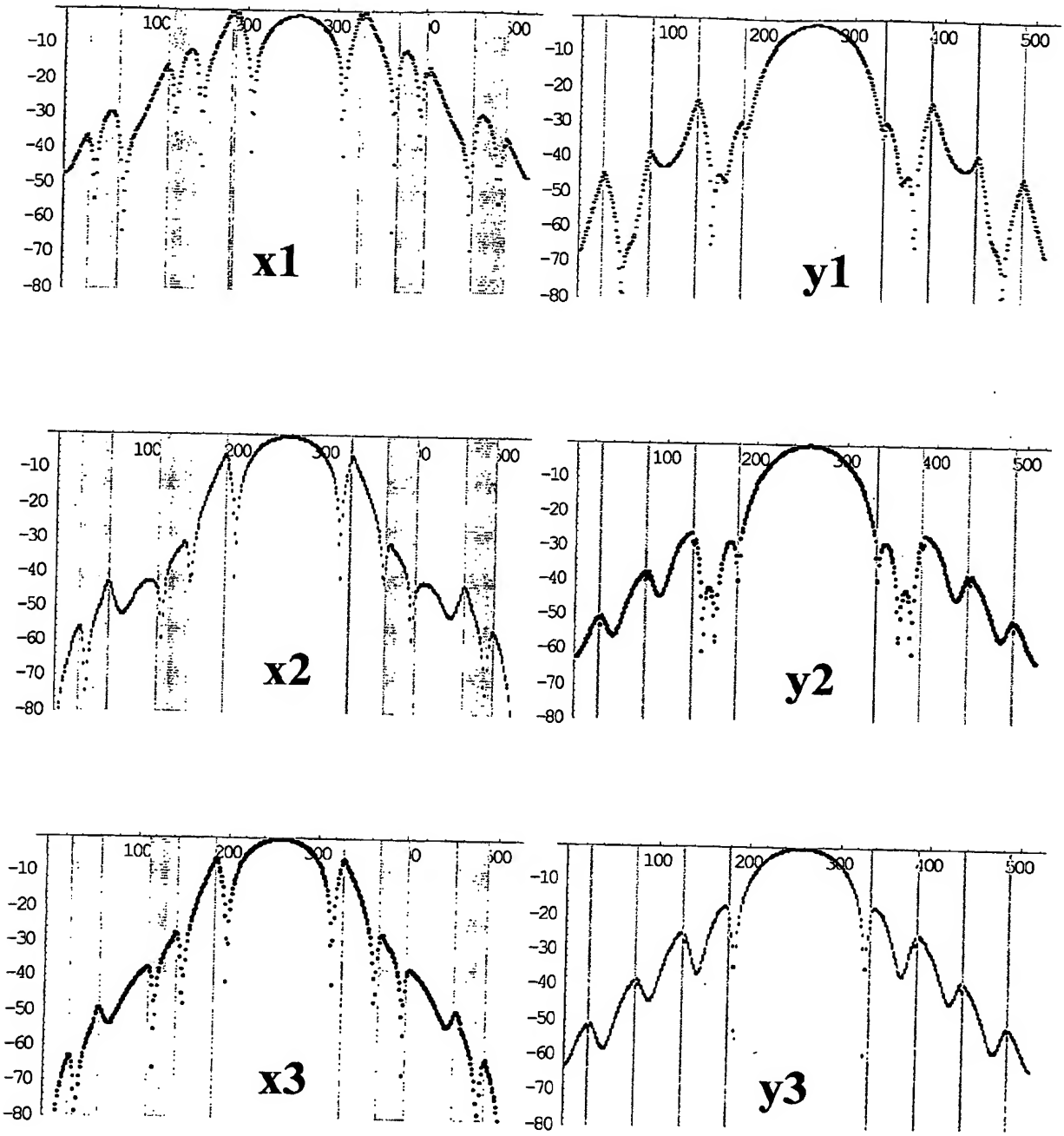

Figure 8

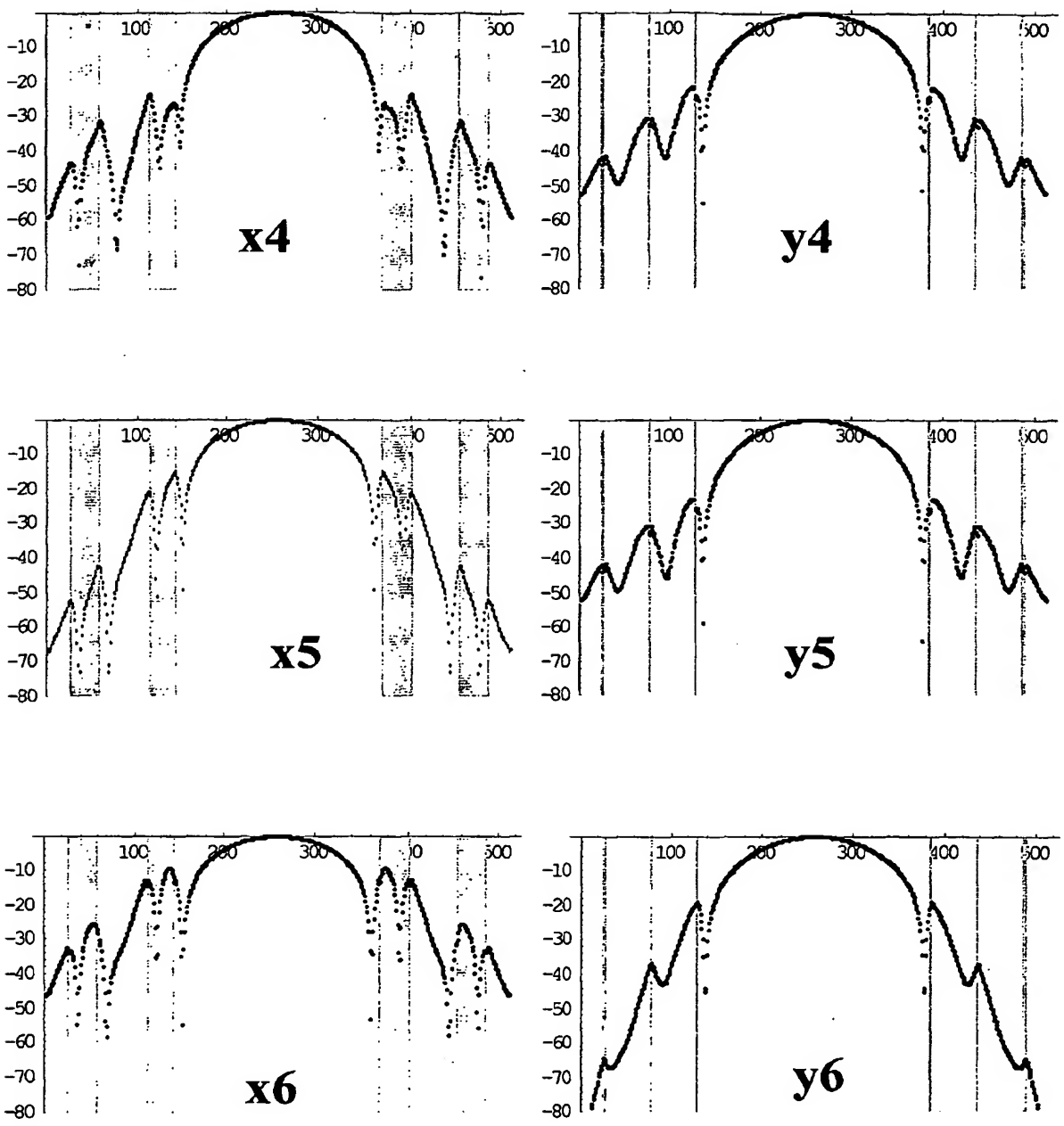

Figure 9

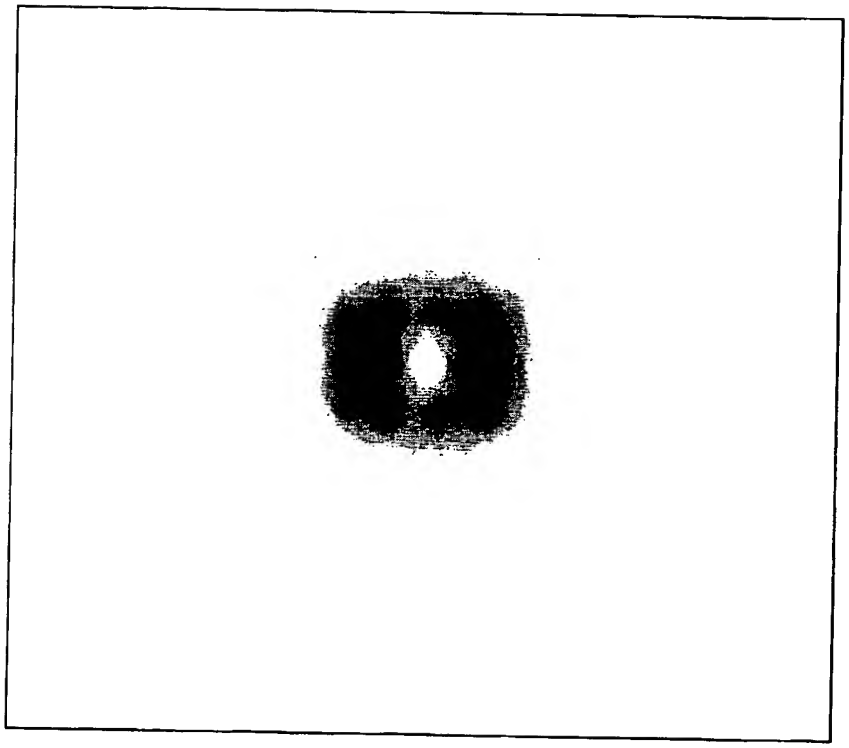

Figure 10

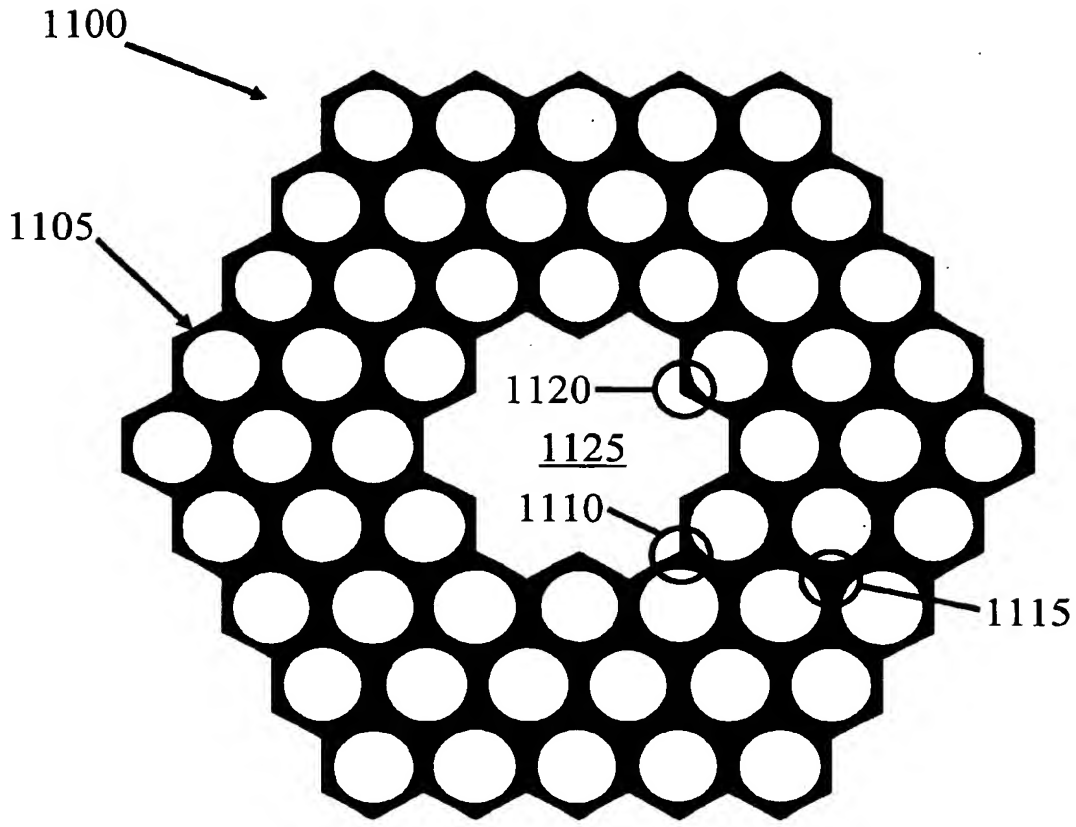

Figure 11

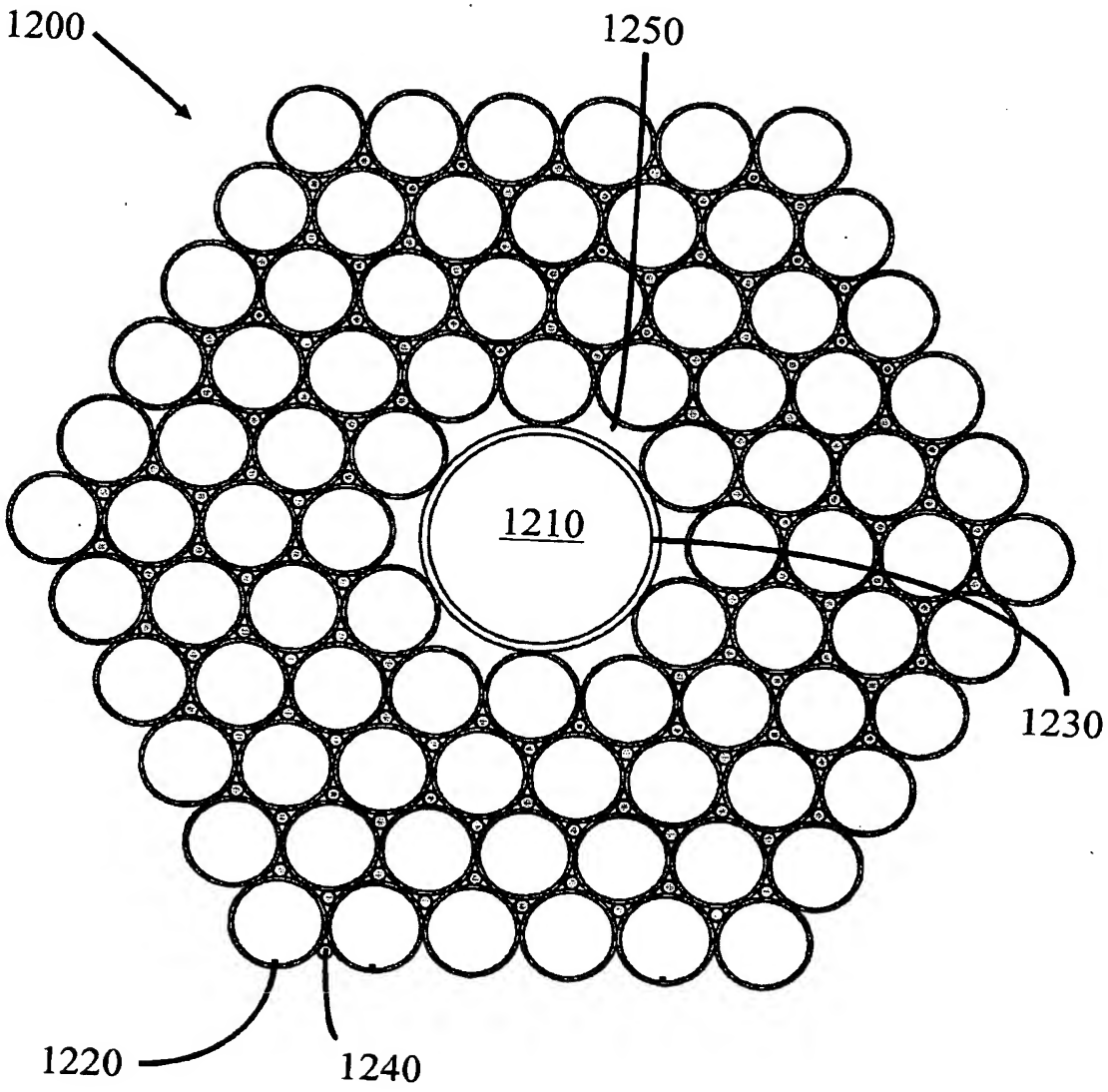

Figure 12

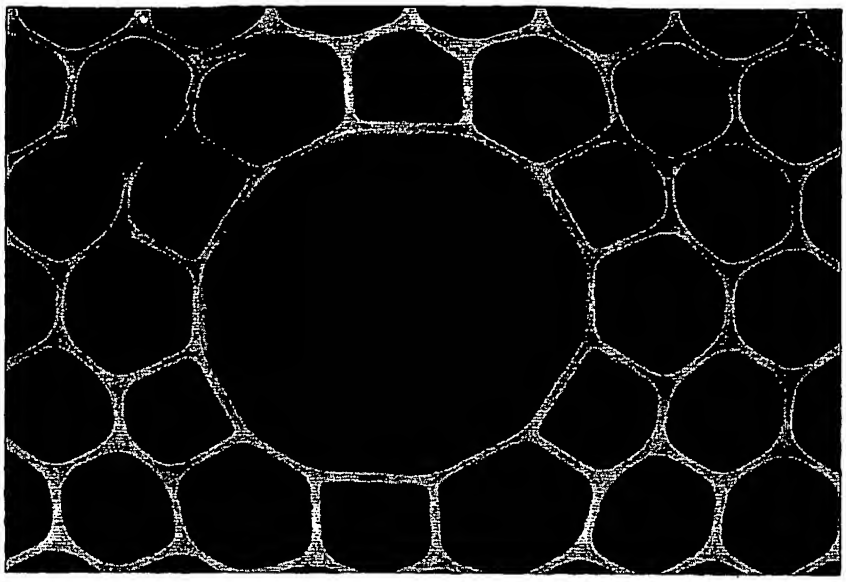

Figure 13a

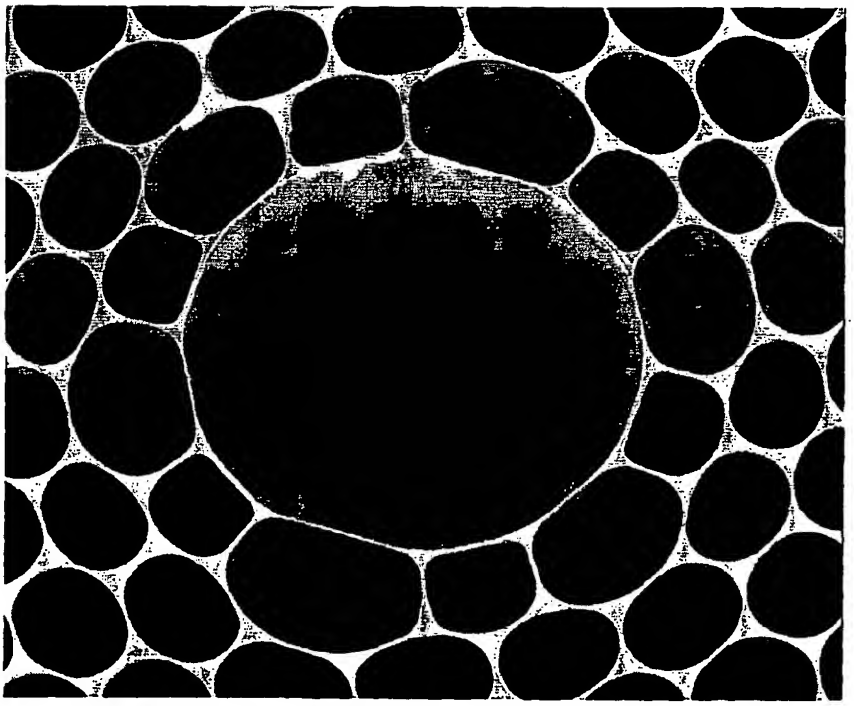

Figure 13b

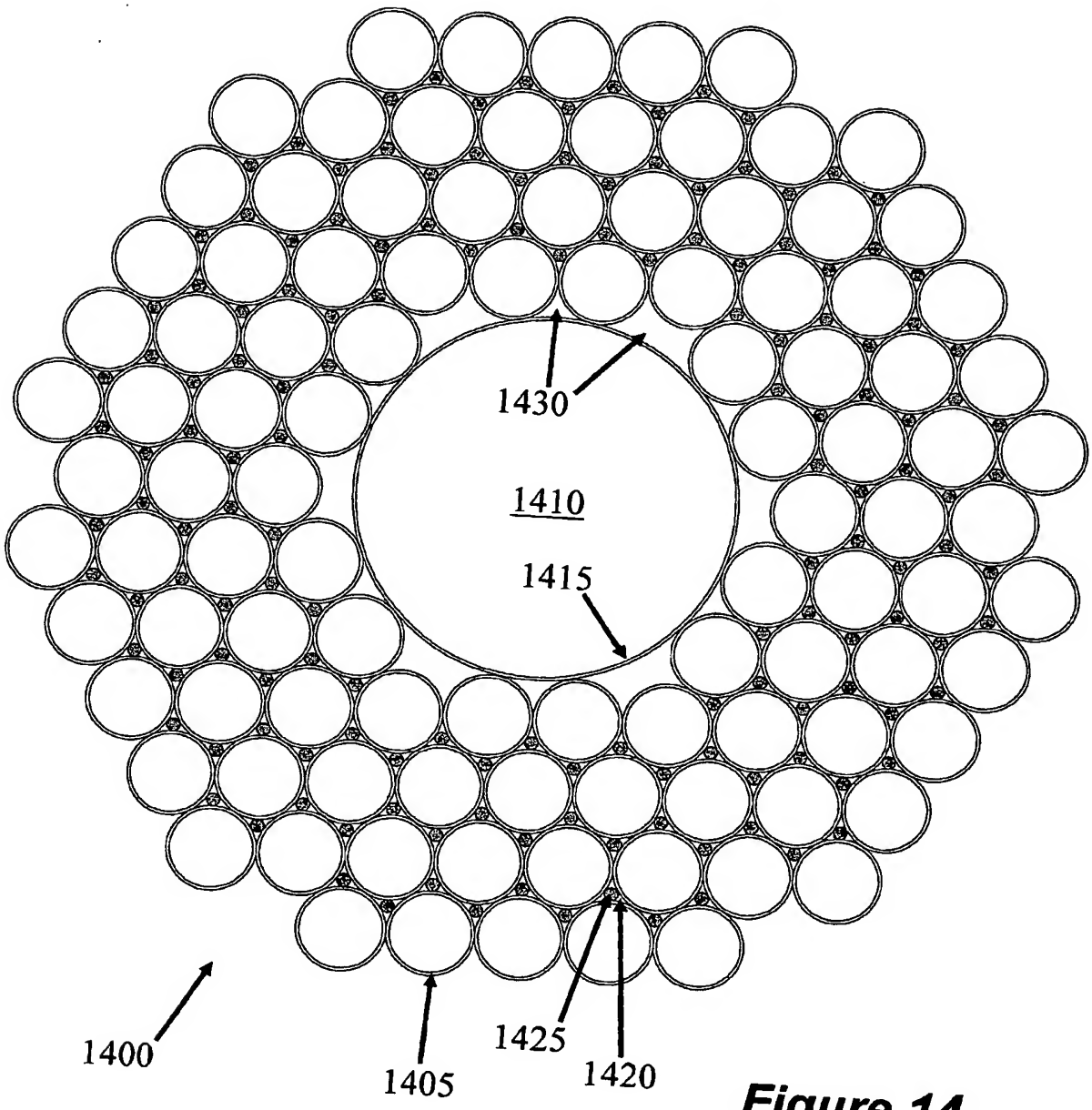

Figure 14

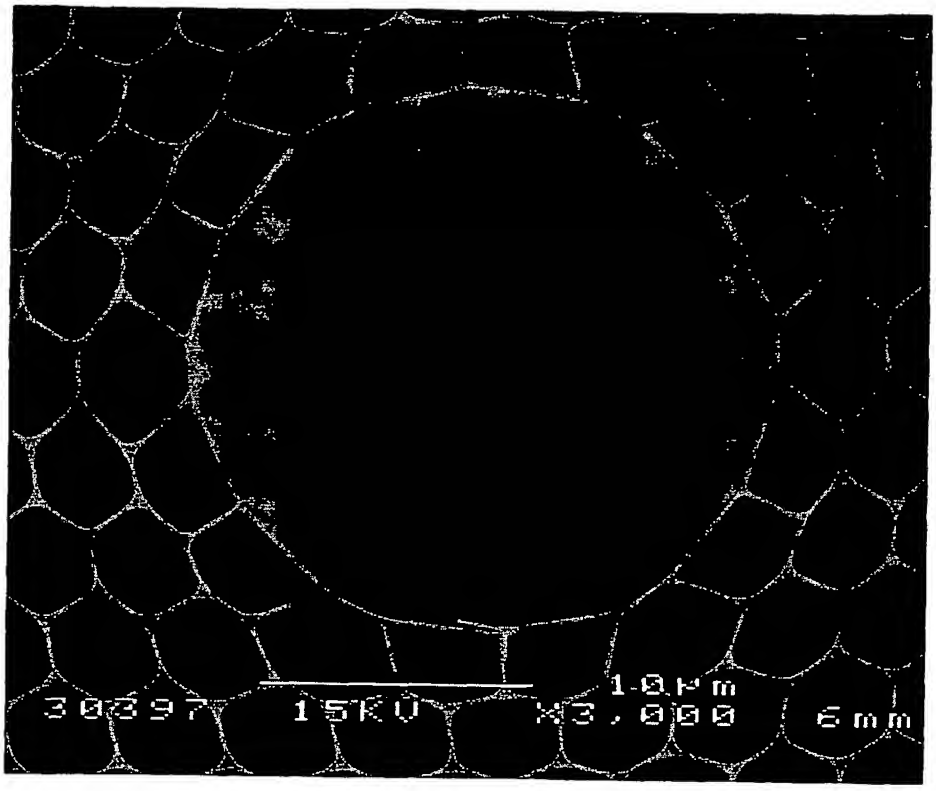

Figure 15

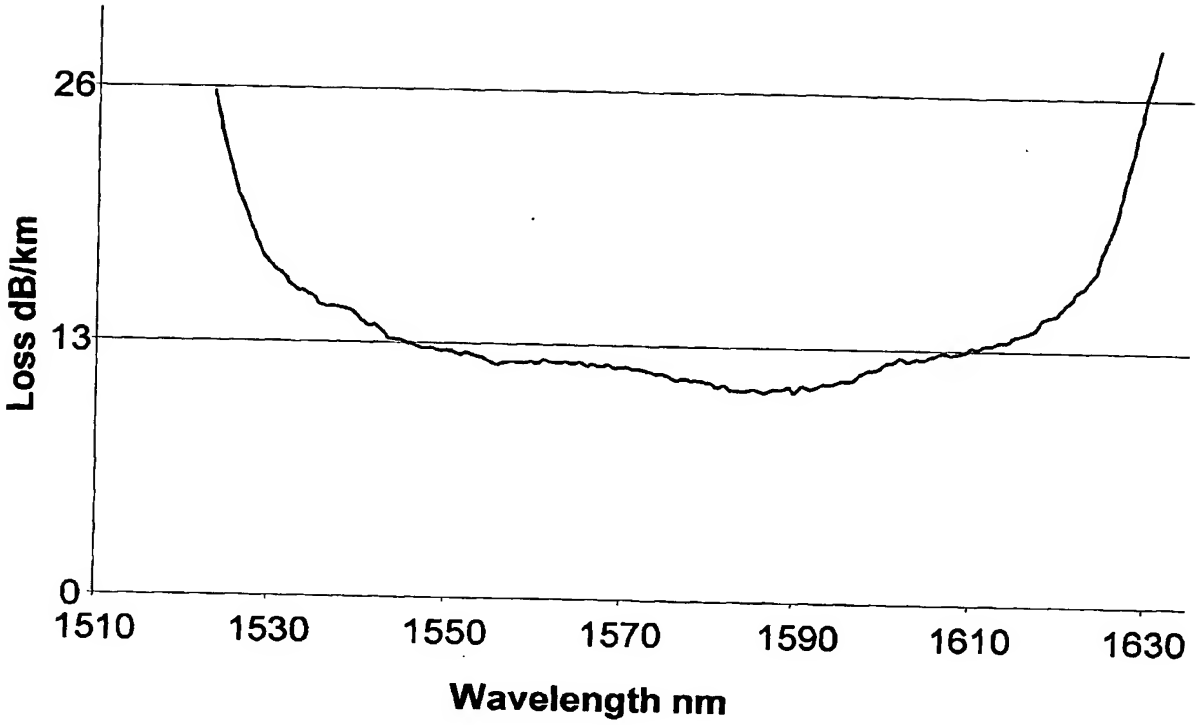
26
13
0
Loss dB/km
1510
1530
1550
1570
1590
1610
1630
Wavelength nm

Figure 16

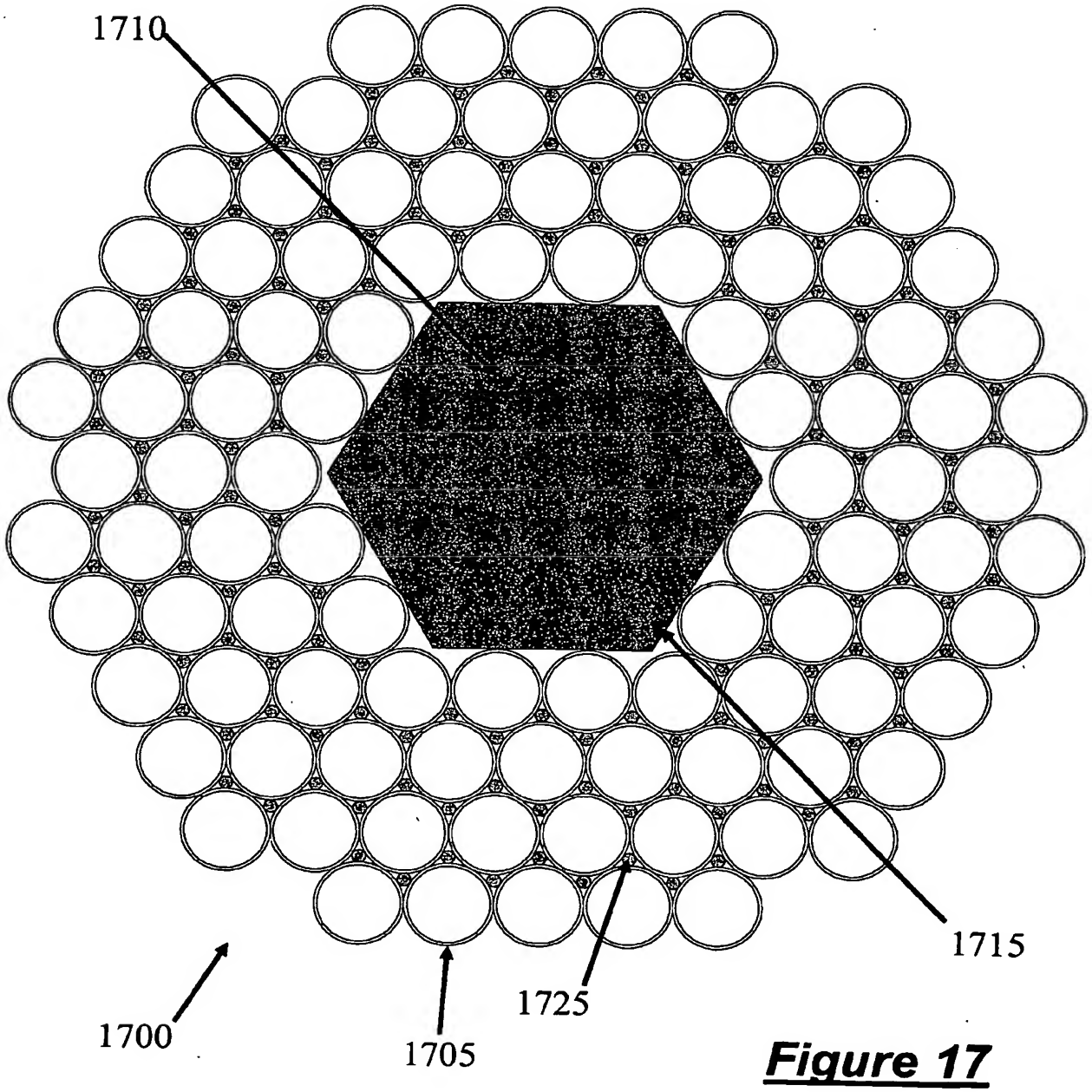

Figure 17

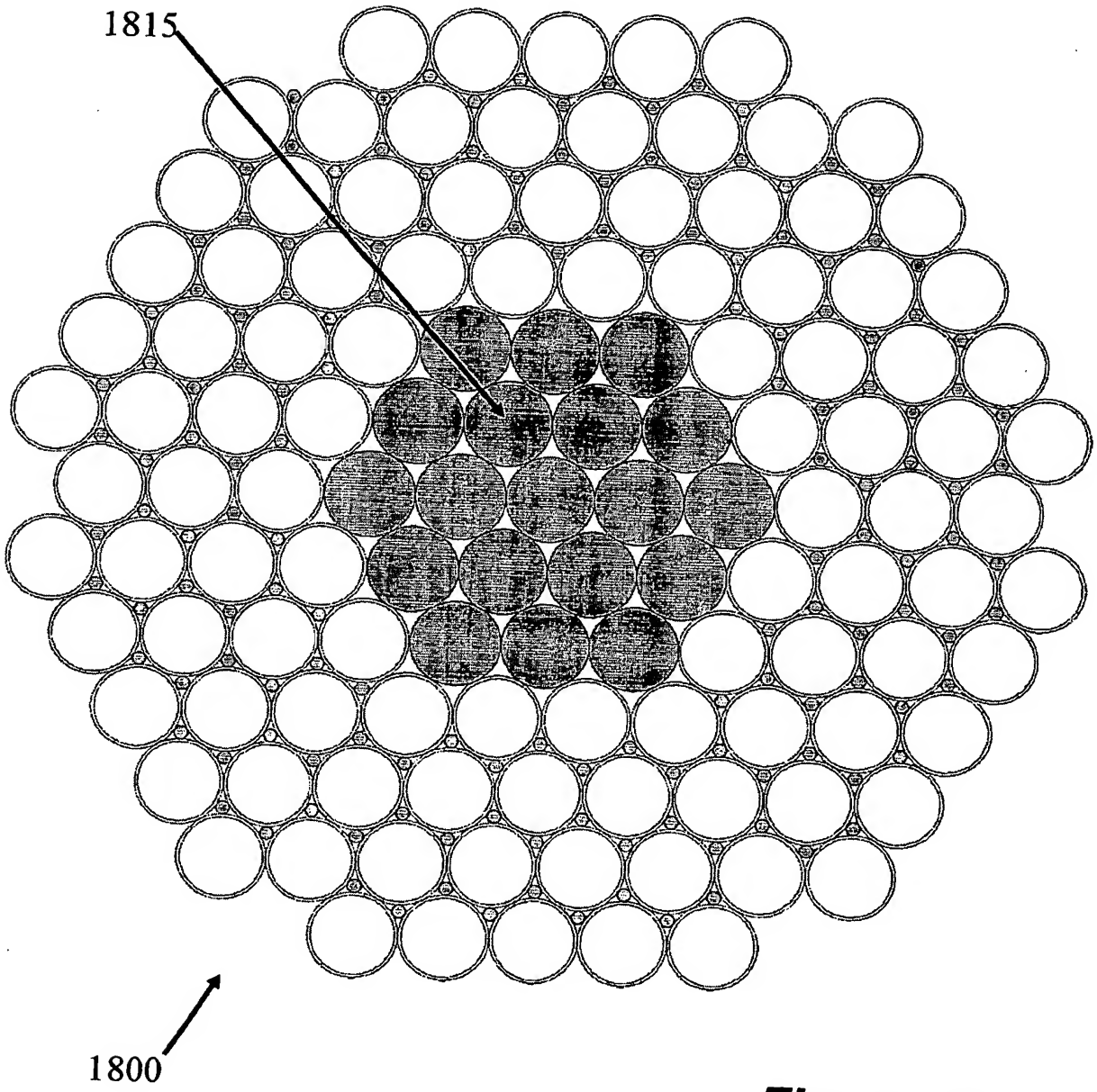

Figure 18

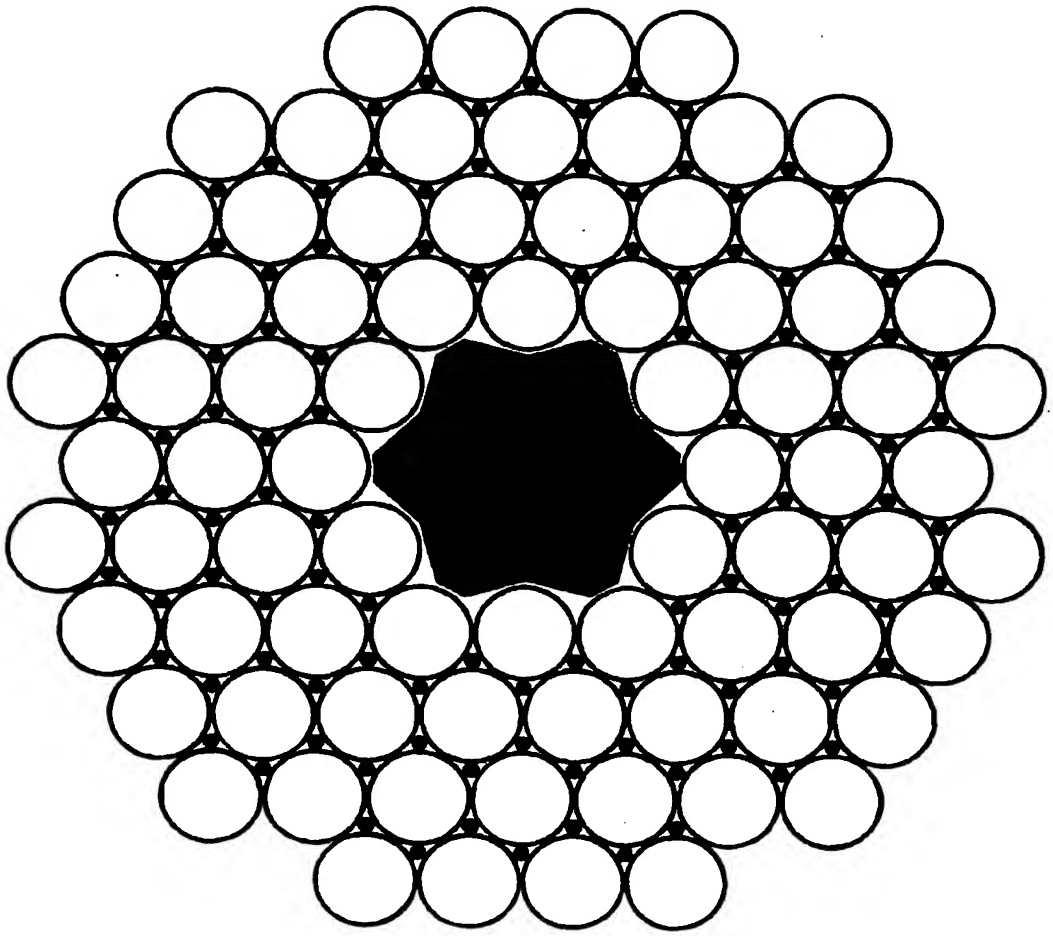

Figure 19

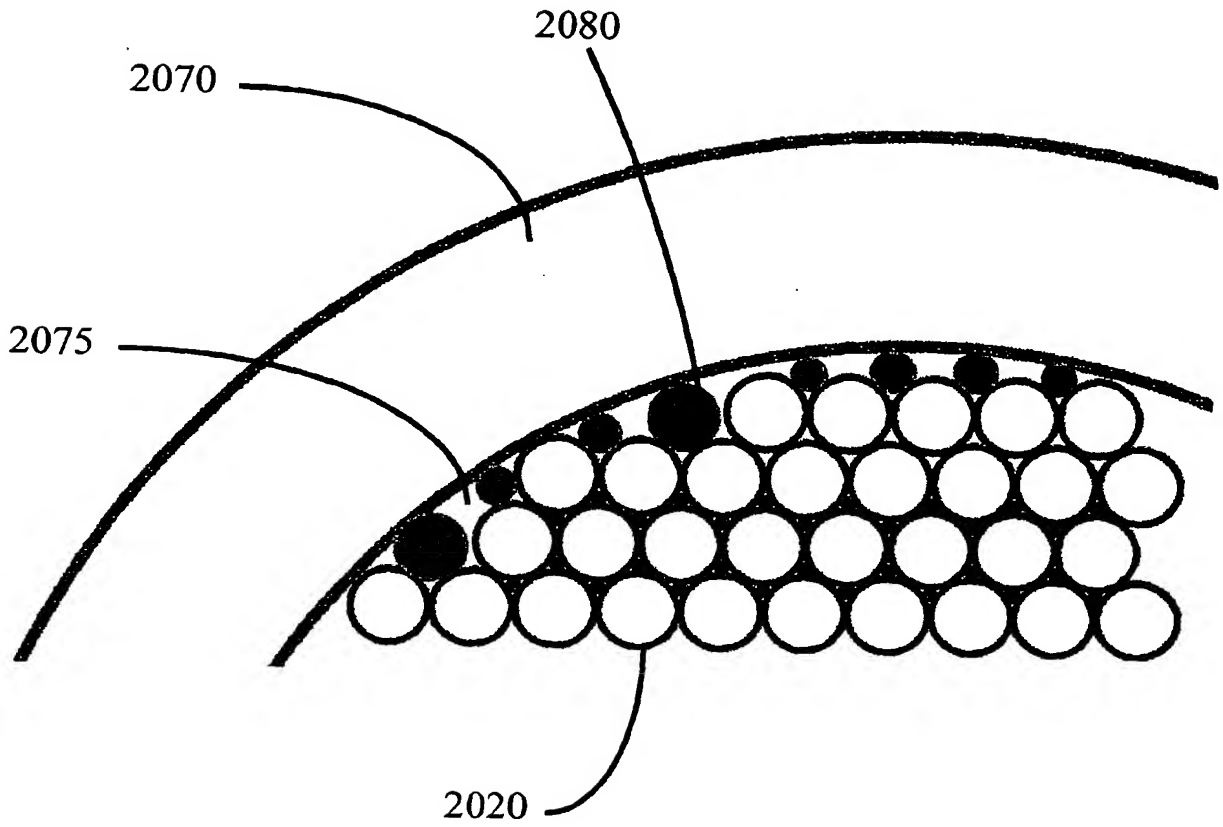

Figure 20

INTERNATIONAL SEARCH REPORT

Inter al Application No
PCT/GB 03/05666

A. CLASSIFICATION OF SUBJECT MATTER
IPC 7 G02B6/16 G02B6/20 C03B37/012

According to International Patent Classification (IPC) or to both national classification and IPC

B. FIELDS SEARCHED

Minimum documentation searched (classification system followed by classification symbols)
IPC 7 G02B C03B

Documentation searched other than minimum documentation to the extent that such documents are included in the fields searched

Electronic data base consulted during the international search (name of data base and, where practical, search terms used)
EPO-Internal, PAJ, INSPEC, COMPENDEX

C. DOCUMENTS CONSIDERED TO BE RELEVANT

Category *	Citation of document, with indication, where appropriate, of the relevant passages	Relevant to claim No.
X	WO 99 64903 A (BARKOU STIG EIGIL ;BJARKLEV ANDERS OVERGAARD (DK); BROENG JES (DK)) 16 December 1999 (1999-12-16) page 9, line 4 - line 14; figure 8 page 12, line 25 page 16, line 11 -page 17, line 27 page 17, line 8 - line 20 page 22, line 27 -page 25, line 28	1-50, 52-77
Y	page 38, line 20 -page 39, line 25; figures 10-13,17-19 page 43, line 22 - line 28	52
Y	WO 00 06506 A (CORNING INC) 10 February 2000 (2000-02-10) page 3	52

-/--

[X] Further documents are listed in the continuation of box C.

[X] Patent family members are listed in annex.

* Special categories of cited documents :

"A" document defining the general state of the art which is not considered to be of particular relevance

"E" earlier document but published on or after the international filing date

"L" document which may throw doubts on priority claim(s) or which is cited to establish the publication date of another citation or other special reason (as specified)

"O" document referring to an oral disclosure, use, exhibition or other means

"P" document published prior to the international filing date but later than the priority date claimed

"T" later document published after the international filing date or priority date and not in conflict with the application but cited to understand the principle or theory underlying the invention

"X" document of particular relevance; the claimed invention cannot be considered novel or cannot be considered to involve an inventive step when the document is taken alone

"Y" document of particular relevance; the claimed invention cannot be considered to involve an inventive step when the document is combined with one or more other such documents, such combination being obvious to a person skilled in the art.

"&" document member of the same patent family

Date of the actual completion of the international search	Date of mailing of the international search report
30 March 2004	21/04/2004

Name and mailing address of the ISA	Authorized officer
European Patent Office, P.B. 5818 Patentlaan 2 NL - 2280 HV Rijswijk Tel. (+31-70) 340-2040, Tx. 31 651 epo nl, Fax: (+31-70) 340-3016	Bourhis, J-F

Form PCT/ISA/210 (second sheet) (January 2004)

INTERNATIONAL SEARCH REPORT

Inte al Application No
PCT/GB 03/05666

C.(Continuation) DOCUMENTS CONSIDERED TO BE RELEVANT

Category *	Citation of document, with indication, where appropriate, of the relevant passages	Relevant to claim No.
X	WO 02 075392 A (CORNING INC) 26 September 2002 (2002-09-26) cited in the application page 6, line 25 - line 28; figures 3,8-10 page 12, line 3 - line 15	1-4, 7-26, 28-38, 40-58, 63, 71-74, 76,77
X	WO 00 60388 A (MANGAN BRIAN JOSEPH ;SECR DEFENCE (GB); BIRKS TIMOTHY ADAM (GB); K) 12 October 2000 (2000-10-12) cited in the application column 8, line 6 -column 9, line 8 column 10, line 30 -column 12, line 15; figures 1-3	11-20, 22-25, 30,32, 34-48, 50, 52-58, 74,76,77
X	US 6 404 966 B1 (OKAMOTO KATSUNARI ET AL) 11 June 2002 (2002-06-11) cited in the application column 4, line 39 -column 5, line 21; figures 5-8	11-20, 22-25, 28-32, 34-38, 40-50, 52-57, 74,76,77
A	KNIGHT J C ET AL: "PHOTONIC BAND GAP GUIDANCE IN OPTICAL FIBERS" SCIENCE, AMERICAN ASSOCIATION FOR THE ADVANCEMENT OF SCIENCE,, US, vol. 282, no. 5393, 20 November 1998 (1998-11-20), pages 1476-1478, XP001009986 ISSN: 0036-8075 page 1476 -page 1478	1-77
A	LITCHINITSER N M ET AL: "ANTIRESONANT REFLECTING PHOTONIC CRYSTAL OPTICAL WAVEGUIDES" OPTICS LETTERS, OPTICAL SOCIETY OF AMERICA, WASHINGTON, US, vol. 27, no. 18, 15 September 2002 (2002-09-15), pages 1592-1594, XP001161774 ISSN: 0146-9592 page 1594	15-29

Form PCT/ISA/210 (continuation of second sheet) (January 2004)

INTERNATIONAL SEARCH REPORT

Inter... ial Application No
PCT/GB 03/05666

Patent document cited in search report		Publication date	Patent family member(s)		Publication date
WO 9964903	A	16-12-1999	AU	755223 B2	05-12-2002
			AU	3026099 A	30-12-1999
			AU	755547 B2	12-12-2002
			AU	3810699 A	30-12-1999
			CA	2334510 A1	16-12-1999
			CA	2334554 A1	16-12-1999
			WO	9964904 A1	16-12-1999
			WO	9964903 A1	16-12-1999
			EP	1086393 A1	28-03-2001
			EP	1086391 A1	28-03-2001
			JP	2002517793 T	18-06-2002
			JP	2002517794 T	18-06-2002
			NZ	509201 A	26-11-2002
			US	6539155 B1	25-03-2003
WO 0006506	A	10-02-2000	AU	5002099 A	21-02-2000
			CA	2339114 A1	10-02-2000
			CN	1311763 T	05-09-2001
			EP	1119523 A1	01-08-2001
			JP	2002521306 T	16-07-2002
			WO	0006506 A1	10-02-2000
			US	6260388 B1	17-07-2001
			US	2001020373 A1	13-09-2001
WO 02075392	A	26-09-2002	EP	1370893 A2	17-12-2003
			TW	539875 B	01-07-2003
			WO	02075392 A2	26-09-2002
			US	2002136516 A1	26-09-2002
WO 0060388	A	12-10-2000	AU	763796 B2	31-07-2003
			AU	3827400 A	23-10-2000
			CA	2368778 A1	12-10-2000
			CN	1353824 T	12-06-2002
			EP	1166160 A1	02-01-2002
			WO	0060388 A1	12-10-2000
			GB	2350904 A ,B	13-12-2000
			JP	2002541507 T	03-12-2002
			NO	20014740 A	03-12-2001
			PL	350990 A1	24-02-2003
US 6404966	B1	11-06-2002	JP	3072842 B2	07-08-2000
			JP	2000035521 A	02-02-2000